

~~SECRET~~

23
487

OAK RIDGE NATIONAL LABORATORY LIBRARY



3 4456 0023199 7

ORNL-1261
Progress
JA

AEC RESEARCH AND DEVELOPMENT REPORT

DECLASSIFIED

CLASSIFICATION CHANGED BY AUTHORITY OF *E. J. Murphy 6.13.62*
BY: *A. S. Bowman 3.14.62*

~~SECRET~~

SOLID STATE DIVISION
QUARTERLY PROGRESS REPORT
FOR PERIOD ENDING JANUARY 31, 1952

LABORATORY RECORDS
1952

58

INV.

50
487

Inv
56



**CENTRAL RESEARCH LIBRARY
DOCUMENT COLLECTION**

LIBRARY LOAN COPY

DO NOT TRANSFER TO ANOTHER PERSON

If you wish someone else to see this document, send in name with document and the library will arrange a loan.

OAK RIDGE NATIONAL LABORATORY
OPERATED BY
CARBIDE AND CARBON CHEMICALS COMPANY
A DIVISION OF UNION CARBIDE AND CARBON CORPORATION

UCC

POST OFFICE BOX P
OAK RIDGE, TENNESSEE

INV.

50
487

~~SECRET~~

~~SECURITY INFORMATION~~

Central Research
Library

COPY NO. 8

ERRATA SHEET
SOLID STATE DIVISION QUARTERLY PROGRESS REPORT
FOR PERIOD ENDING JANUARY 31, 1952
ORNL 1261

PAGE NO.	COLUMN NO.	LINE NO.	ERRATA
26	1	13	<i>Replace "The measurement of" with "Measurements of neutron energy spectra, used together with the results from radiation damage experiments, permit a better understanding of the fundamental relationship between energies of bombarding neutrons and characteristics of damage produced."</i>

[REDACTED]

ORNL-1261

This document consists of 56 pages.
Copy 8 of 147 copies. Series A.

Contract No. W-7405-eng-26

SOLID STATE DIVISION
QUARTERLY PROGRESS REPORT
for Period Ending January 31, 1952

D. S. Billington, Director

Edited by
J. T. Howe

DATE ISSUED

SEP 25 1952

[REDACTED]

OAK RIDGE NATIONAL LABORATORY
Operated by
CARBIDE AND CARBON CHEMICALS COMPANY
A Division of Union Carbide and Carbon Corporation
Post Office Box P
Oak Ridge, Tennessee

[REDACTED]



3 4456 0023199 7

[REDACTED]

INTERNAL DISTRIBUTION

1. G. T. Felbeck (C&CCC)
- 2-3. Chemistry Library
4. Physics Library
5. Biology Library
6. Health Physics Library
7. Metallurgy Library
- 8-9. Training School Library
10. Reactor Experimental Engineering Library
- 11-14. Central Files
15. C. E. Center
16. C. E. Larson
17. W. B. Humes (K-25)
18. L. B. Emler (Y-12)
19. A. M. Weinberg
20. E. H. Taylor
21. E. J. Murphy
22. E. D. Shipley
23. D. S. Billington
24. F. C. VonderLage
25. R. C. Briant
26. J. A. Swartout
27. S. C. Lind
28. F. L. Steahly
29. A. H. Snell
30. A. Hollaender
31. M. T. Kelley
32. G. H. Clewett
33. K. Z. Morgan
34. J. S. Felton
35. A. S. Householder
36. C. S. Harrill
37. C. E. Winters
38. D. W. Cardwell
39. E. M. King
40. C. P. Keim
41. L. K. Jetter
42. E. J. Boyle
43. W. D. Manly
44. C. D. Susano
45. B. S. Borie
46. R. J. Gray
47. E. E. Stansbury
48. G. P. Smith
49. J. E. Cunningham
50. E. C. Miller
51. A. Brasunas
52. A. G. H. Andersen
53. J. O. Betterton, Jr.
54. R. B. Oliver
55. P. Patriarca
56. T. H. Blewitt
57. J. H. Crawford, Jr.
58. W. E. Brundage
59. O. Sisman
60. G. W. Keilholtz
61. J. T. Howe
62. R. H. Kernohan
63. S. E. Dismuke
64. J. C. Wilson
65. W. J. Sturm
66. M. T. Robinson
67. A. F. Cohen
68. J. W. Cleland
69. K. Lark-Horovitz (Consultant)
70. M. C. Wittels
71. R. A. Weeks
72. W. W. Parkinson
73. C. D. Bopp
74. C. D. Baumann
75. J. B. Trice
76. J. G. Morgan

- [REDACTED]
- | | |
|-------------------------|-----------------------------|
| 77. G. E. Klein | 82. R. S. Livingston (Y-12) |
| 78. R. G. Berggren | 83. R. J. Jones (Y-12) |
| 79. D. K. Holmes | 84. D. D. Cowen |
| 80. D. K. Stevens | 85. P. M. Reyling |
| 81. A. J. Miller (Y-12) | |

EXTERNAL DISTRIBUTION

- 86-93. Argonne National Laboratory
- 94-96. Atomic Energy Commission, Washington
- 97-100. Brookhaven National Laboratory
- 101-104. Carbide and Carbon Chemicals Company (Y-12 Area)
- 105-107. Knolls Atomic Power Laboratory
- 108-109. General Electric Company, Richland
- 110. Hanford Operations Office
- 111-114. Los Alamos *
- 115-116. New York Operations Office
- 117. Patent Branch, Washington
- 118-132. Technical Information Service, Oak Ridge
- 133-136. University of California Radiation Laboratory
- 137. Massachusetts Institute of Technology (Kaufmann)
- 138. Battelle Memorial Institute
- 139-141. North American Aviation, Inc.
- 142. Westinghouse Electric Corporation
- 143. Savannah River Operations Office, Wilmington
- 144-147. Idaho operations office (1 copy to Phillips Petroleum)

[REDACTED]

Reports previously issued in this series are as follows:

ORNL-1025	Period Ending January 31, 1951
ORNL-1095	Period Ending April 30, 1951
ORNL-1128	Period Ending July 31, 1951
ORNL-1214	Period Ending October 31, 1951

[REDACTED]

[REDACTED]

[REDACTED]

PUBLICATIONS

The following articles have appeared in open publications during the past quarter:

J. W. Cleland, J. H. Crawford, Jr., K. Lark-Horovitz, J. C. Pigg, and F. W. Young, Jr., "Evidence for Production of Hole Traps in Germanium by Fast Neutron Bombardment," *Phys. Rev.* 84, 861 (Nov. 15, 1951).

J. C. Pigg, "A Multirange Recording and Control System for Electrical Measurements," *Science* 114, 667 (Dec. 21, 1951).

[REDACTED]

[REDACTED]

TABLE OF CONTENTS

	Page
INTRODUCTION AND SUMMARY	1
SOLID STATE REACTIONS	5
Position of Bombardment-produced Energy Levels in Germanium	5
Installation of Arthur D. Little Magnet	7
Magnetic Susceptibility of Neutron-bombarded Germanium	7
Stored Energy Measurements at Elevated Temperatures	9
Cryostat for Pile Irradiations	10
RADIATION METALLURGY	10
Effect of Precipitate Nuclei on Electrical Resistivity of Copper-Beryllium Alloy	10
Use of Retrogression Phenomena to Resolve Particles Affecting Resistivity from Those Affecting Hardness	10
Effect of Irradiation on Subsequent Aging of Copper-Titanium Alloy	12
Irradiation of Supersaturated Solid Solutions in the LITR	13
Beta Phase Copper-Beryllium Alloy	13
Creep Under Irradiation	13
Radiation Damage to Ferromagnetic Materials	18
An Evaluation of Temperature Controllers	18
Radiation Damage to Dielectrics	19
Impact Tests on Irradiated Steel	20
ENGINEERING PROPERTIES	21
X-10 Graphite Pile Liquid-Metals Loop	21
Liquid-Metals Stress-Corrosion Loop	21
MTR Fluoride-Fuel Loop	22
Physical Properties of Irradiated Plastics and Elastomers	23
Pile-induced Radiation in Materials of Construction	26
Measurement of Neutron Energy Spectra	26
LIQUID FUELS	32
Radiation Damage to Liquid Fuels	32
CRYSTAL PHYSICS	37
Y-12 Cyclotron Radiation Damage Studies	37
Correlation of Neutron Bombardment with Proton Bombardment	38

[REDACTED]

	Page
X-ray Work	39
Thermal Conductivity of Structural Materials	40
SPECIAL PROJECTS	41
Tests on Graphite-Uranium Oxide Bars	41
Activity Measurements of Special Materials	43
Irradiation of Diamond Chips	43

[REDACTED]

[REDACTED]

[REDACTED]

[REDACTED]

LIST OF FIGURES

FIGURE	TITLE	PAGE
1	Initial Hole Concentration vs. Initial Slope at -196°C	6
2	Initial Hole Concentration vs. Initial Slope at -78°C	7
3	Initial Hole Concentration vs. Initial Slope at 27°C	7
4	ADL Electromagnet	8
5	Stored-Energy Calorimeter	9
6	Change of Critical Nucleus Size with Temperature (Schematic)	10
7	Hypothetical Nucleated Condition Showing the Range of Size Affecting Resistance (A) and Hardness (B)	11
8	Hypothetical Retrogression Curves Illustrating Resolution Between Particle Sizes	11
9	Effect of Temperature on Maximum Resistance Increase During Aging of Copper-Beryllium Alloy	12
10	Radiation Effect on Aging of Copper-Titanium Alloy at 200°C	12
11	Radiation Effect on Aging of Copper-Titanium Alloy at 125°C	12
12	Radiation Effect on Aging of Copper-Titanium Alloy at 400°C After Prior Aging at 125°C	13
13	Radiation Effect on Aging of Copper-Titanium Alloy at 400°C After Prior Aging at 200°C	13
14	Comparison of Bench and Inpile Creep Curves	15
15	Comparison of Bench and Inpile Creep Rates	16
16	Effect of Pile Power on Output Voltage and Leakage Resistance of Schaevitz Model 18-LCT Microformer	17

FIGURE	TITLE	PAGE
17	System Used in Testing Controllers (Schematic)	19
18	Optimum Performance of Air and PAT Controllers	19
19	Impact Strength of Irradiated ASTM Type A-70 Steel	20
20	Compression Jig	25
21	Top View of LITR (Schematic)	27
22	Neutron Energy Spectrum in LITR Pneumatic Rabbit Tube (North Lower Center Reactor Lattice)	28
23	High Energy Region of Neutron Energy Spectrum in LITR Pneumatic Rabbit Tube	28
24	Two Neutron Density Energy Spectra in LITR	29
25	Decay Curves for P^{32} and Si^{31} from P^{31}	29
26	Decay Curves for Al^{28} , Mg^{27} , and Na^{24} from Al^{27}	30
27	Decay Curves for Na^{24} and Cl^{38} from $Na^{23}Cl^{37}$	30
28	Decay Curves for V^{52}	31
29	Capsule and Heater Assembly	33
30	Temperature and Radiation Effect on Pressure of Potassium Hydroxide in X-10 Graphite Pile, Hole 12	33
31	Potassium Hydroxide in Type-316 Stainless Steel Capsule Under Irradiation	34
32	Potassium Hydroxide in Type-316 Stainless Steel Capsule Unirradiated	35
33	Metallograph of No. 2 Reactor Fuel Capsule Exposed in X-10 Graphite Pile	35
34	Metallograph of No. 2 Reactor Fuel Capsule Exposed in LITR	35
35	Graphite-Uranium Oxide Specimen Container	43

SOLID STATE DIVISION QUARTERLY PROGRESS REPORT

INTRODUCTION AND SUMMARY

This report covers work performed in the Solid State Division for the period November 1, 1951, to January 31, 1952.

SOLID STATE REACTIONS

Position of Bombardment-produced Energy Levels in Germanium. The James-Lehman model of energy levels associated with lattice defects has been expressed in a form using chemical equilibrium constants, and the initial rate of change of hole concentration with disorder has been calculated for a number of temperatures and energy-level positions. This initial change has been compared with experimental data.

Installation of Arthur D. Little Magnet. The ADL electromagnet, which was ordered more than a year ago, has been installed in the basement of Building 3025. Fields of 24,000 gauss may be obtained over a 2-in. gap with a pole-face diameter of 5 3/4 inches. The gap width is adjustable in 1/8-in. steps from 1/8 in. to 4 inches.

Magnetic Susceptibility of Neutron-bombarded Germanium. A sensitive balance is being constructed for the purpose of measuring the magnetic susceptibility of unirradiated and irradiated germanium. The balance is expected to be capable of measuring micrograms of force, and it is hoped that the presence of 10^{17} unpaired electrons per cubic centimeter will be detectable.

Stored Energy Measurements at Elevated Temperatures. The energy stored in most materials suffering radiation damage has been found to be of low order as measured by the physical property changes. Additional measurements of stored energy will be conducted by using thermal methods. A design has been developed for a high-sensitivity calorimeter that will have a low thermal inertia to allow rapid temperature changes and which will detect energy changes as small as 0.01 cal/g. The calorimeter will accommodate solid cylindrical specimens 1/4 in. in diameter by 1/4 in. in length.

Cryostat for Pile Irradiations. The cryostat project was inactive except for some machine shop work.

RADIATION METALLURGY

Effect of Precipitate Nuclei on Electrical Resistivity of Copper-Beryllium Alloy. The charge distribution in the vicinity of a precipitate platelet is being examined to determine the sensitivity of the charge distribution to the shape of the potential well. Results are not yet available.

Use of Retrogression Phenomena to Resolve Particles Affecting Resistivity from Those Affecting Hardness. On the basis of the theory that different physical properties are affected by different sizes of nuclei, it may be possible to separate particles affecting resistivity from those affecting hardness. The change in physical properties may be observed when the specimens are heated to various temperatures so that all nuclei smaller than the critical size are dispersed.

Since retrogression begins at critical temperature, resistivity and hardness curves will exhibit the retrogression phenomena at different temperatures.

Present data indicate that resistance measurements are sensitive to the size of the nucleus, whereas hardness depends largely on lattice strain; these data are not yet considered conclusive, since hardness measurements have not been reproducible.

Effect of Irradiation on Subsequent Aging of Copper-Titanium Alloy. The investigation of the effect of irradiation on subsequent aging of copper-titanium alloys after solution-quenching has been extended to the lower temperatures of 200 and 125°C. As in previous experiments at higher temperatures, irradiation decreases the subsequent rate of precipitation as measured by electrical resistance. Further aging at 400°C produces about the same rate of change in the irradiated specimens as in the unirradiated specimens.

SOLID STATE DIVISION QUARTERLY PROGRESS REPORT

Irradiation of Supersaturated Solid Solutions in the LITR. An investigation of the increase in electrical resistance of supersaturated solid solutions as a function of integrated power has been initiated in the LITR. Present data indicate an increase of about 16% for an exposure of copper-beryllium specimens for one month.

Copper-titanium and aluminum-silicon alloys are also being investigated; hardness and resistance measurements are being used.

Beta Phase Copper-Beryllium Alloy. No further information has been obtained on the x-ray investigation of the beta phase copper-beryllium alloy that is being conducted in cooperation with the x-ray group of the Metallurgy Division.

Creep Under Irradiation. A determination of inpile cantilever creep rates on type-347 stainless steel at 8000 psi was made at various temperatures in the X-10 graphite pile. Creep rates varied by a factor of 1200 over a temperature range from 1200 to 1400°F. Dual bench tests under the same conditions are not yet complete.

Comparison of a 500-hr before-after test of type-347 stainless steel at 1500°F and 1500 psi in the X-10 graphite pile with its bench counterpart disclosed that the strain of the bench test is 5% greater. This is contrary to expected results based on extrapolation of past data. Another test that was run under the same conditions, except for a shorter period of time, and in which an extensometer was utilized, showed a sharp increase in creep rate after about 200 hr in the pile. Both experiments will be repeated.

Results of inpile tests on electrolytic nickel at 2000 psi and 1300°F confirmed previous observations made on type-347 stainless steel at 1500°F that in the earlier stage the creep rate diminishes faster under irradiation but becomes constant quicker and at higher rates than it does in the absence of radiation.

Inconel tests at 1500°F and 1500 psi have been started. Results are not yet complete.

Further studies were made on the behavior of microformers used in measuring cantilever creep.

Primary-to-secondary leakage seems to account for the output voltage change with pile power. It is recommended that measurement of interwinding leakage should replace or supplement the proposal that leakage resistance to ground be used as a criterion for indication of inpile microformer breakdown.

The check on accuracy of the thermocouples used in creep tests has also been continued. Equipment has been built to use sodium chloride and possibly an alloy system having a melting point of about 1500°F for these calibrations.

Preparations are also being made for conducting creep tests in the LITR and the MTR. A new type of extensometer utilizing a Bourdon tube is under consideration for measurements in these tests.

Radiation Damage to Ferromagnetic Materials. Specimens of magnetic materials that represent a range of initial permeability have been obtained. The effect of radiation damage on the magnetic properties of these materials will be studied, with emphasis placed on the effects these changes might have on microformers.

An Evaluation of Temperature Controllers. An evaluation of temperature controllers for use with the tensile creep rig in the MTR is in progress. The dummy specimen contains a heater to simulate gamma heating. Thus far, controls appear to be adequate, but a long-term stability study of the controllers will be continued.

Radiation Damage to Dielectrics. Plans are being formed to run before-after and inpile tests on the effects of irradiation on dielectrics. High-frequency characteristics of cables sheathed in the dielectric materials will be of particular interest. The first of the dielectrics will be received in April.

Impact Tests on Irradiated Steel. The study of radiation effects on construction materials of interest to the Homogeneous Reactor Project has been started, with emphasis given to the impact testing of steels. ASTM type A-70 steel that had been irradiated at Hanford was tested first at temperatures from -112 to +302°F. A considerable decrease in strength was noted.

Radiation effects on the impact strength of a number of metals of interest to the HRP will be studied in the future.

ENGINEERING PROPERTIES

X-10 Graphite Pile Liquid-Metals Loop. A liquid-metals loop was operated in the X-10 graphite pile for a period of two weeks. A stoppage occurred at the end of the first week, but it was relieved by alternate applications of pressure and vacuum. At the end of the second week another stoppage occurred that could not be relieved. Total operation of the loop with the pile on was 115 hr at 1500°F and 50 hr at 1000°F. Decay curves are being examined for evidence of long-life corrosion products from the inconel tube walls. An attempt to determine the cause of the stoppages will be made as soon as the activity decreases sufficiently.

Liquid-Metals Stress-Corrosion Loop. Fabrication of the inpile stress-corrosion loop is about 80% complete and instrumentation is ready. The gas displacement pump for use with the loop was tested on a glass system and is now being modified to run with liquid sodium for flow calibration and study of its behavior at operating temperature.

MTR Fluoride-Fuel Loop. A design is being prepared for a dynamic corrosion experiment circulating a fused fluoride fuel. This apparatus is intended to operate in the MTR. The purposes of the experiment will be to obtain data on corrosion and heat transfer characteristics of the system and to discover what other problems exist in such a system at high fluxes. The amount of fission xenon that will accumulate may also be measured.

Physical Properties of Irradiated Plastics and Elastomers. Samples of plastics and elastomers were placed in evacuated glass capsules and irradiated in the X-10 graphite pile. The amount of gas given off by the plastics appears to be in direct proportion to the degree of physical property change for the plastics reported, except in the case of Styron 475. This observation does not hold true for elastomers, many of which gave off no gas even though they exhibited large changes in physical properties.

A number of new elastomers specially compounded by the B. F. Goodrich Company Research Center were tested. Those compounded for use as gasket materials were irradiated while under pressure and compared to bench tests subjected to the same conditions but without irradiation.

Pile-induced Radiation in Materials of Construction. No new materials have been added to this project. A topical report will be published soon.

Measurement of Neutron Energy Spectra. The neutron energy spectra and the fast-neutron flux have been measured in the LITR at the center of the upper pneumatic rabbit hole 5 1/4 in. from a fuel element and separated from the element by a beryllium piece. The ratio of total integrated flux above thermal energies to total thermal flux at the same location is 0.31 as compared to 0.55 for hole 19 of the X-10 graphite pile. Above 1 Mev the ratio in the LITR is 0.056 as compared with 0.034 for hole 19 of the X-10 graphite pile.

LIQUID FUELS

Radiation Damage to Liquid Fuels. A facility has been prepared in beryllium piece C-48 in the LITR for exposure of liquid fuels to radiation. This facility will normally prorate 1.2×10^{13} neutrons/cm² as compared with the 8.0×10^{11} neutrons/cm² in hole 12 of the X-10 graphite pile. Potassium hydroxide and several fused fluoride salts were tested.

The test on potassium hydroxide in C-48 indicated a pressure increase of 3 psi, which was attributed to the water content in the potassium hydroxide since the control sample produced the same increase.

After 115 hr in C-48, reactor fuel No. 2, which consists of 46.5 mole % NaF, 26.0 mole % KF, and 27.5 mole % UF₄, showed a corrosion increase by a factor of 10 (by chemical analysis) when compared with previous X-10 graphite pile and 86-in. cyclotron runs; metallographic examination indicated an increase by a factor of 3 to 6. No pressure effects were observed during irradiation.

SOLID STATE DIVISION QUARTERLY PROGRESS REPORT

Reactor fuels No. 3 (60 mole % BeF_2 , 25 mole % NaF , 15 mole % UF_4) and No. 17 (51 mole % BeF_2 , 47 mole % NaF , 2 mole % UF_4) were irradiated, but examination of the data is not complete.

Work is in progress on the design and fabrication of apparatus to permit extension of these tests to the higher flux that will be available in the MTR.

CRYSTAL PHYSICS

Y-12 Cyclotron Radiation Damage Studies. Proton bombardments of 20 Mev were made on a number of liquid fuels and coolants to test radiation effects on the liquids and their containers. All targets were water-cooled.

Neither inconel nor type-316 stainless steel capsules (0.010-in. walls) that contained KOH held up under 2 to 3 μa of protons at 650°C.

Bombardments of UF_4 eutectics were made in inconel capsules of two designs. The eutectics contained 27 and 1.1 mole % UF_4 , respectively.

Chemical analyses and metallurgical studies are not yet complete.

Correlation of Neutron Bombardment with Proton Bombardment. In order to obtain a better comparison between the damage done by proton bombardment in the cyclotron and the damage done by neutron bombardment in reactors, several polycrystalline copper targets were bombarded in the cyclotron and elastic limits were determined. It is estimated that 1×10^{18} nvt corresponds to about 2 $\mu\text{a}\text{-hr}/\text{cm}^2$. By using this correlation, 25 $\mu\text{a}/\text{cm}^2$ proton irradiation would produce effects 1000 times as fast as the X-10 graphite pile or 60 times as fast as the LITR.

Calculated values using a $1/E$ spectrum indicate 1×10^{18} nvt = 0.5 $\mu\text{a}\text{-hr}/\text{cm}^2$, which agrees within the limits of error with the experimental value.

X-Ray Work. X-ray studies were made of lithium fluoride crystals before and after irradiation; no change was observed in lattice parameter. It was

found that lines of wave lengths other than normal appear when strongly diffracting materials such as lithium fluoride are used in a well-aligned spectrometer producing high-intensity x rays.

Operation of the G-E x-ray tube for the hot cell spectrometer and the North American Phillips diffraction tube using power from the Hilger unit was not successful. The tubes require high d-c voltage; a North American Phillips unit will be used as the power source in the future.

Apparatus has been built for the study of small-angle scattering produced by the refraction of x rays passing through thin foils of metal crystals. An effort will be made to obtain direct evidence of the formation of precipitate nuclei after irradiation of copper-beryllium alloy.

The radiation background on the first floor of the Solid State Building has become too high to permit film storage in the building. It has also been necessary to provide the Geiger tube of the Norelco spectrometer with a 1/4-in. lead shield; even so, the portion of the spectrometer trace below 350 counts/min is unobtainable.

Thermal Conductivity of Structural Materials. Thermal conductivity measurements have been made on inconel, nickel, and type-316 stainless steel in the X-10 graphite pile and the LITR. Temperatures at which measurements were made varied from 200 to 820°C. The only observed change was in inconel; this material showed no change up to 575°C, but at 820°C in the X-10 graphite pile a decrease was noted. Inconel that has been stabilized with respect to carbide precipitation up to 850°C is now being run in the LITR.

SPECIAL PROJECTS

Tests on Graphite-Uranium Oxide Bars. Pre-irradiation measurements of weight, modulus of elasticity, relative thermal conductivity, and electrical resistivity were made on the graphite-uranium oxide test bars fabricated by Battelle Memorial Institute. These specimens will be

irradiated for one month each in hole B of the X-10 graphite pile at an approximate thermal flux of 9×10^{11} neutrons/cm².

Activity Measurements of Special Materials. A number of insulator samples and aluminum and platinum samples were exposed for 108 hr in hole 1968 of the X-10 graphite pile, and the beta and gamma activity was measured with a cutie pie held

in contact with the specimen. This work was requested by GE-ANP, and the results have been tabulated.

Irradiation of Diamond Chips. Preparations are being made to irradiate diamond chips in the LITR and MTR. An attempt will be made to correlate change in the lattice constant of diamond with the integrated fast flux.

SOLID STATE REACTIONS

POSITION OF BOMBARDMENT-PRODUCED ENERGY LEVELS IN GERMANIUM

J. H. Crawford J. W. Cleland

The James-Lehman model of energy levels associated with Frenkel defects in germanium⁽¹⁾ has been examined and re-expressed in a form more amenable for comparison with experimental data. In this model the lattice disorder introduces hole traps and electron traps in equal concentration below the middle of the forbidden energy band. The hole concentration for any extent of disorder (for any bombardment period) in P-type germanium is given by

$$n_h = n_h^0 + N_a^- - N_d^+ + n_e, \quad (1)$$

where n_h^0 is the initial hole concentration from chemical impurities that are considered to be completely ionized, N_a^- is the concentration of ionized acceptors or low-lying electron traps, N_d^+ is the concentration of ionized hole traps, and n_e is the concentration of electrons present by virtue of intrinsic excitation. Usually it is possible to neglect n_e for P-type material in which n_h is appreciable. The values of N_a^- and N_d^+ may be obtained from the mass action law

$$\frac{n_h N_a^-}{N_a - N_a^-} = K_1,$$

⁽¹⁾K. Lark-Horovitz, "Nucleon-Bombarded Semi-conductors," *Semi-conducting Materials*, p. 47, esp. p. 74, Academic Press, Inc., New York, 1951.

$$K_1 = \left[\frac{2(2\pi mkT)^{3/2}}{h^3} \right] e^{-\Delta\epsilon_1/kT} \quad (2)$$

and

$$\frac{N_d^+}{(N_d - N_d^+)n_h} = K_2,$$

$$K_2 = \left[\frac{h^3}{2(2\pi mkT)^{3/2}} \right] e^{\Delta\epsilon_2/kT}, \quad (3)$$

where N_a and N_d are the total concentrations of the introduced states, K_1 and K_2 are the equilibrium constants for the two processes, and $\Delta\epsilon_1$ and $\Delta\epsilon_2$ are the ionization energy and the hole trap depth, respectively. In this treatment it is convenient to use the relation $\Delta\epsilon_1 > \Delta\epsilon_2$. Replacing N_a^- and N_d^+ in Eq. 1 with their values from Eqs. 2 and 3 and setting $N_a = N_d = N$ gives

$$\begin{aligned} n_h^3 K_2 + n_h^2 (1 + K_1 K_2 - n_h^0 + K_2 N) \\ + n_h (K_1 - n_h^0 - K_1 K_2 n_h^0) \\ - K_1 (n_h^0 + N) = 0. \quad (4) \end{aligned}$$

SOLID STATE DIVISION QUARTERLY PROGRESS REPORT

The variation of n_h with N is given by

$$\frac{dn_h}{dN} = \frac{K_1 - K_2 n_h^2}{K_2 n_h^2 + n_h(1 + K_1 K_2 - n_h^0 + K_2 N) + K_1 - n_h^0 - K_1 K_2 n_h^0} \quad (5)$$

At saturation $dn_h/dN = 0$. Thus

$$(n_h)_{\text{limit}} = \left(\frac{K_1}{K_2}\right)^{1/2} = \left[\frac{2(2\pi mkT)^{3/2}}{h^3}\right] e^{-(\Delta\epsilon_1 + \Delta\epsilon_2)/2kt} \quad (6)$$

Hence it is evident that the limiting value of the Fermi level is

$$\zeta_{\text{limit}} = \frac{\Delta\epsilon_1 + \Delta\epsilon_2}{2} \quad (7)$$

in agreement with the result of James and Lehman.

Equation 5 has been used to calculate the initial slope $(dn_h/dN)_i$ as a function of n_h^0 for a variety of $\Delta\epsilon_1$ and $\Delta\epsilon_2$ values and for three temperatures under the conditions $N = 0$ and $n_h = n_h^0$. ζ_{limit} was chosen by interpolation of initial slopes measured at -78°C ; the value used was 0.15 ev. The results of these calculations are shown in Figs. 1, 2, and 3. At each temperature five activation energies were used; their values in electron volts were as follows:

- I. $\Delta\epsilon_1 = 0.275$,
 $\Delta\epsilon_2 = 0.025$,
- II. $\Delta\epsilon_1 = 0.250$,
 $\Delta\epsilon_2 = 0.050$,
- III. $\Delta\epsilon_1 = 0.200$,
 $\Delta\epsilon_2 = 0.100$,
- IV. $\Delta\epsilon_1 = 0.175$,
 $\Delta\epsilon_2 = 0.125$,

$$\begin{aligned} \text{V. } \Delta\epsilon_1 &= 0.225, \\ \Delta\epsilon_2 &= 0.075. \end{aligned}$$

The most reliable initial slope data of n_h as a function of $(nvt)_{\text{fast}}$ were taken at -78°C . Assuming the relation

$$\frac{dn_h}{dN} = C \frac{dn_h}{d(nvt)_{\text{fast}}} \quad (8)$$

holds during the initial part of the bombardment where C is the number of traps produced per incident neutron, the experimental data can be plotted for comparison. The experimental points are represented by circles in Fig. 3 where $C = 3.2$. These data fall closest to the curve calculated on the basis of $\Delta\epsilon_1 = 0.225$ ev and $\Delta\epsilon_2 = 0.075$ ev. Since the value of C used in this comparison may be in error by as much as a factor of 2, the values of $\Delta\epsilon_1$ and $\Delta\epsilon_2$ should not be taken with complete confidence.

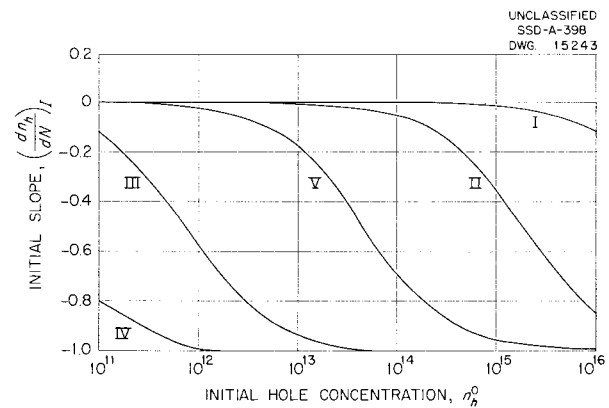


Fig. 1. Initial Hole Concentration vs. Initial Slope at -196°C .

It should be pointed out that a discrete energy value for the two types of disorder-produced states is assumed for this model. There is evidence from the Hall coefficient and resistivity data measured as a function of temperature on bombarded ger-

manium that there may be a distribution of these states in energy. If this is true, calculations from this model are expected to have only semiquantitative value. The parameters of the model are now being determined directly from experimental curves, and from these results the validity of the model can be more adequately decided.

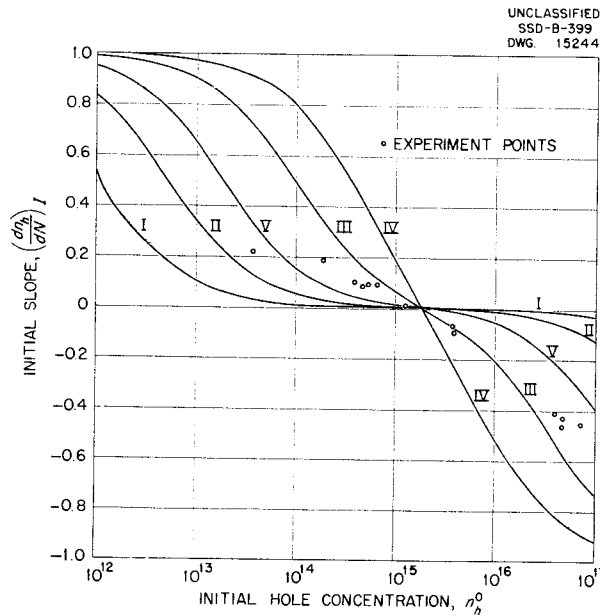


Fig. 2. Initial Hole Concentration vs. Initial Slope at -78°C .

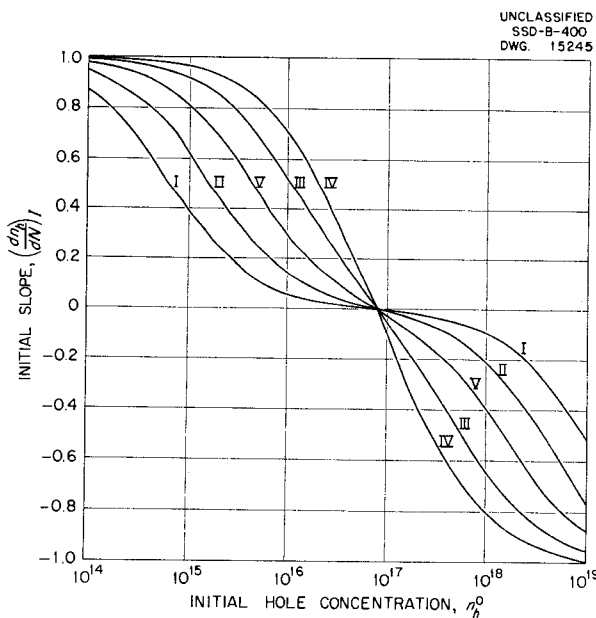


Fig. 3. Initial Hole Concentration vs. Initial Slope at 27°C .

INSTALLATION OF ARTHUR D. LITTLE MAGNET

J. W. Cleland J. H. Crawford
J. C. Pigg

The large electromagnet ordered from Arthur D. Little, Inc. over a year ago has arrived and has been installed in Building 3025. This magnet is very efficient; with a 25-kw power source, fields up to 24,000 gauss are obtainable over a 2-in. gap with a pole-face diameter of 5 3/4 inches. The installation of the magnet represents a large portion of the effort of the Solid State Reactions group during the past quarter, and the instrument is now available as a division facility for studying the effect of radiation damage on the magnetic properties of solids.

A view of the magnet with the yokes separated in order to give an idea of the design is shown in Fig. 4. The efficiency of operation is largely due to the design for the return path of the magnetic current. A shell of iron that completely surrounds the pole pieces provides the return path. Access to the gap is made possible by four ports, 6 by 6 in. square. The gap width is adjustable in 1/8-in. steps from 1/8 in. to 4 in. by means of spacers that are attached to the periphery of the yoke. A rotating coil gauss meter is supplied with the instrument, and the magnetic field can be read directly to an accuracy of 1% on a panel meter. A heat exchanger, which can dissipate up to 100 kw and uses trichlorobenzene as the primary coolant and water as the secondary coolant, is also furnished with the magnet.

MAGNETIC SUSCEPTIBILITY OF NEUTRON-BOMBARDED GERMANIUM

D. K. Stevens

In attempting to settle definitely the question concerning the nature and concentration of energy

SOLID STATE DIVISION QUARTERLY PROGRESS REPORT

states localized around bombardment-produced lattice defects, it becomes necessary to know something concerning the nature of the electrons occupying these states. One means of studying this problem is from the standpoint of the magnetic moment of the trapped electrons. If the trapped electron is unpaired, it will contribute to the paramagnetic susceptibility of the material an amount proportional to two Bohr magnetons. In addition, careful measurement of the temperature dependence of this contribution may indicate the type of binding of the electron in the localized state.

A project is now under way to study the effect of bombardment on the magnetic susceptibility of germanium. A sensitive balance has been constructed that is capable of measuring $10 \mu\text{g}$ of force. The design of the balance is essentially

that used by Hutchinson and Reekie⁽²⁾ as modified by McGuire and Lane.⁽³⁾ The balance arm is mounted rigidly to the center of a beryllium-copper alloy strip, the ends of which are clamped to upright supports. The restoring force applied to offset the unknown load is supplied by the interaction between the speaker magnet and a measured current flowing through a 5-in. speaker coil mounted on the balance beam. In the present design, the mirror and optical system for indication of balance has been replaced by a linear variable differential transformer. This innovation will permit detection of rotation of a 1 1/2-in. balance arm through 10^{-5} radians.

(2) T. S. Hutchinson and J. Reekie, "An Electrodynamical Balance for the Measurement of Magnetic Susceptibilities," *J. Sci. Instruments* 23, 209 (1946).

(3) T. R. McGuire and C. T. Lane, "Magnetic Susceptibility Balance for Use at Liquid Helium Temperatures," *Rev. Sci. Instruments* 20, 489 (1949).

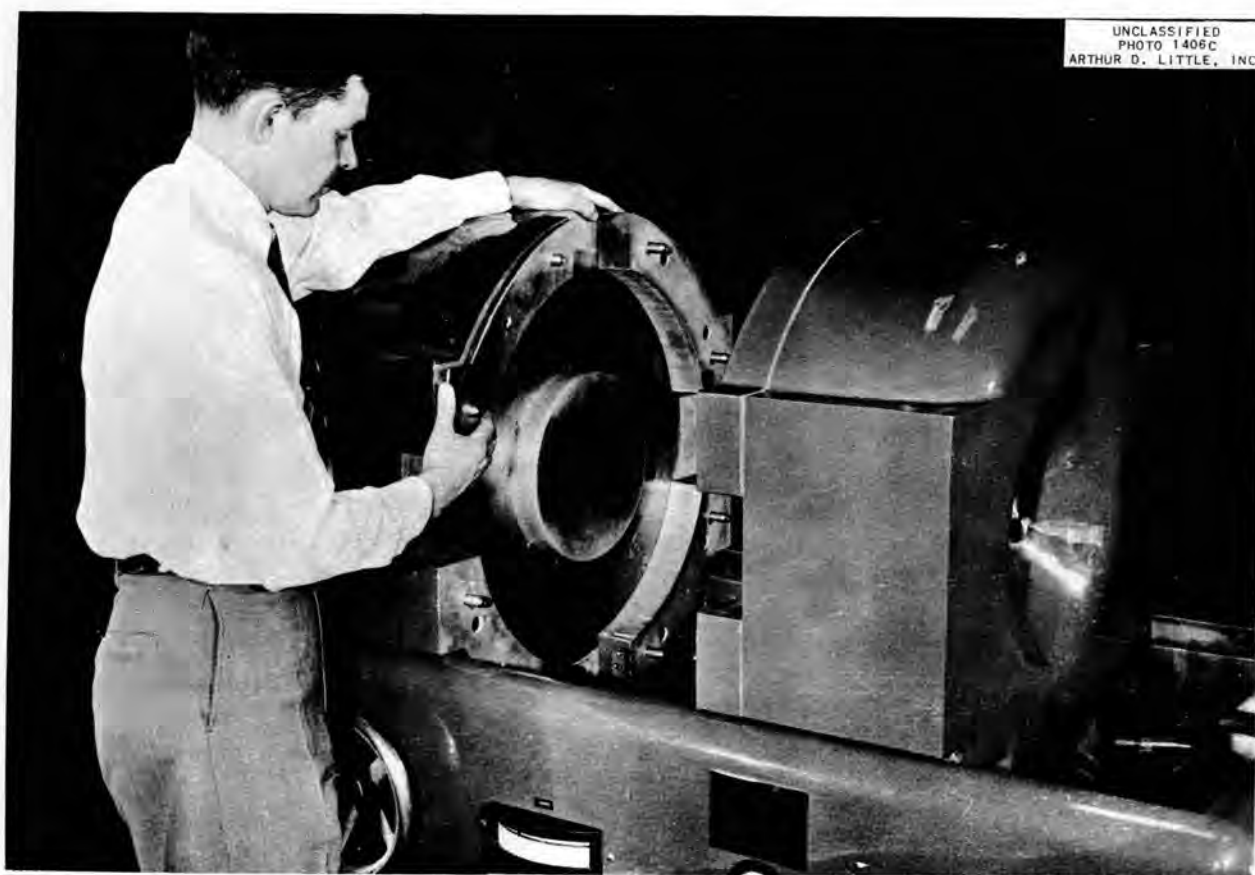


Fig. 4. ADL Electromagnet. Open position, showing removable pole piece and spacers. Fixed height model. (Courtesy Arthur D. Little, Inc.)

The balance will be enclosed in a vacuum system, and susceptibility measurements will be made by using the Arthur D. Little electromagnet.

STORED ENERGY MEASUREMENTS AT ELEVATED TEMPERATURES

M. C. Wittels

It is believed that the magnitude of the energy stored in materials that suffer radiation damage is of a low order; consequently, thermal apparatus for measuring this energy must have a high sensitivity. For this reason an apparatus is under construction that will detect energy changes as small as 0.01 cal/g over short ranges of temperature.

The method of analysis is an adaptation of Sykes' thermal method⁽⁴⁾ that includes the following variations: (1) a calorimeter system of low thermal inertia for use at high rates of heating and cooling, (2) precalibration of the apparatus by means of standard energy transformations in the temperature range 20 to 1250°C, and (3) automatic recording of the thermal curves with the aid of a photoelectric instrument.

The apparatus for this investigation is comprised of three sections: (1) the furnace and crucible, shown in Fig. 5, (2) the recorder, and (3) the furnace controller.

A simple resistance-wound radiation-type furnace that requires approximately 500 w input at 1250°C has been constructed of inconel and nickel. It may be employed at heating rates as high as 40°C/min in vacuum.

The crucible is made from thin-walled lavite designed so that thermal losses from the specimens are largely eliminated. Holes for three chromel-alumel thermocouples are symmetrically placed in the bottom of the crucible equidistant from the furnace wall. Two of these thermocouples are connected in series opposed and make contact

with the test and dummy specimens in the crucible cavities. The differential thermocouple leads are fed into a reflecting galvanometer that forms part of the recording system. Chromel-alumel thermocouples are used in the differential circuit primarily because of their high thermal emf in the 0 to 1000°C range. They are carefully matched and tested in the furnace before any final thermal curves are obtained. The test and dummy specimens are in the form of solid cylinders 1/4 in. long and 1/4 in. in diameter. For materials having densities approaching 9 this volume contributes a mass of about 3 grams.

The evolution or absorption of heat by the test specimen produces a thermal emf that deflects the reflecting galvanometer that is suspended 3 m from the recording instrument. A high-intensity light beam directed on the galvanometer mirror is reflected toward the photocells of a Beckman Photopen Recorder. The arc-chord length difference at a radius of 3 m is less than 0.1% for a 25-cm chord interception. As a result, the recorded deflections are approximately proportional to the current and voltage in the circuit, and the null method of reading is avoided as long as there is

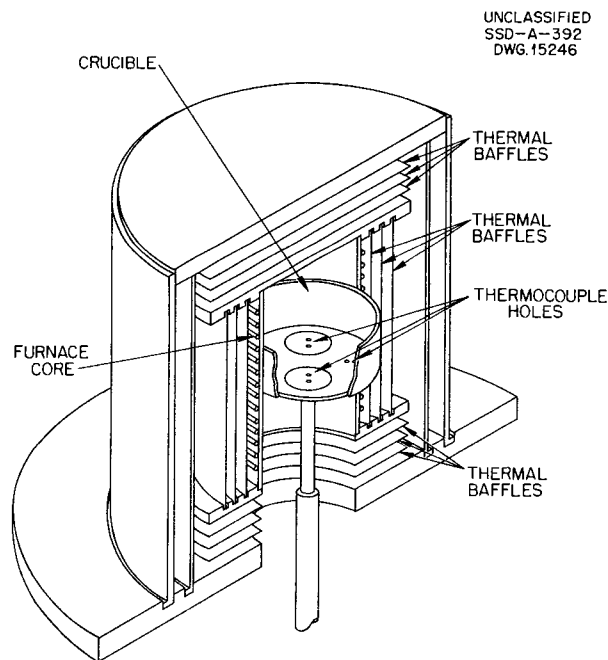


Fig. 5. Stored-Energy Calorimeter.

(4) C. Sykes, "Methods for Investigating Thermal Changes Occurring During Transformations in a Solid Solution," *Proc. Roy. Soc. (London)* A148, 422 (1935).

SOLID STATE DIVISION QUARTERLY PROGRESS REPORT

but one deflection per run. Obviously, the magnitude of the deflections is directly proportional to the galvanometer-photocell distance. With a 3-m distance the deflection magnitude is three times that obtained with the standard 1-m distance.

The furnace is to be controlled by a Leeds and Northrup Program Controller having maximum up-scale and downscale drives of $2500^{\circ}\text{C}/\text{hr}$ in the temperature range 0 to 1400°C . The controller thermocouple and the two differential thermocouples are located in the crucible at equal distances from the furnace wall.

CRYOSTAT FOR PILE IRRADIATIONS

J. T. Howe

No time has been devoted to this project during this quarter other than some machine shop work that was done to replace the helium line vacuum jacket between the cold case and the cryostat proper. With the diffusion pump off, the cryostat section together with the vacuum header can be pulled down to a $12\text{-}\mu$ reading on a National Research thermocouple gage located in the header on the cryostat side of the diffusion pump.

RADIATION METALLURGY

EFFECT OF PRECIPITATE NUCLEI ON ELECTRICAL RESISTIVITY OF COPPER-BERYLLIUM ALLOY

W. E. Taylor G. T. Murray

In previous reports^(1,2) the charge distribution in the vicinity of a precipitate platelet has been estimated on the assumption that the ionic perturbation can be approximated by a square potential well. In order to estimate the sensitivity of the charge distribution to the shape of the potential well the problem is being examined by the application of perturbation theory to the square-well solutions. Results are not yet available.

USE OF RETROGRESSION PHENOMENA TO RESOLVE PARTICLES AFFECTING RESISTIVITY FROM THOSE AFFECTING HARDNESS

W. E. Taylor G. T. Murray

According to the theory of nucleation in solid solutions, for any given temperature and composition there is a minimum size nucleus that is

(1) W. E. Taylor and J. S. Koehler, "Effect of Precipitate Particles on Resistivity of Cu-Be Alloys," *Physics of Solids Institute Quarterly Progress Report for Period Ending July 31, 1951*, ORNL-1128, p. 24.

(2) W. E. Taylor and D. K. Holmes, "Effect of Precipitate Nuclei on Resistivity of a Copper-Beryllium Alloy," *Physics of Solids Institute Quarterly Progress Report for Period Ending October 31, 1951*, ORNL-1214, p. 19.

stable. This critical size increases with increasing temperature, as shown schematically in Fig. 6. If the different properties such as resistivity, hardness, density, etc. are affected primarily by nuclei within a given size range, and if this size range is not the same for the different properties, then the possibility exists of resolution between the sizes. This may be done by establishing a

UNCLASSIFIED
SSD-A-349
DWG. 15247

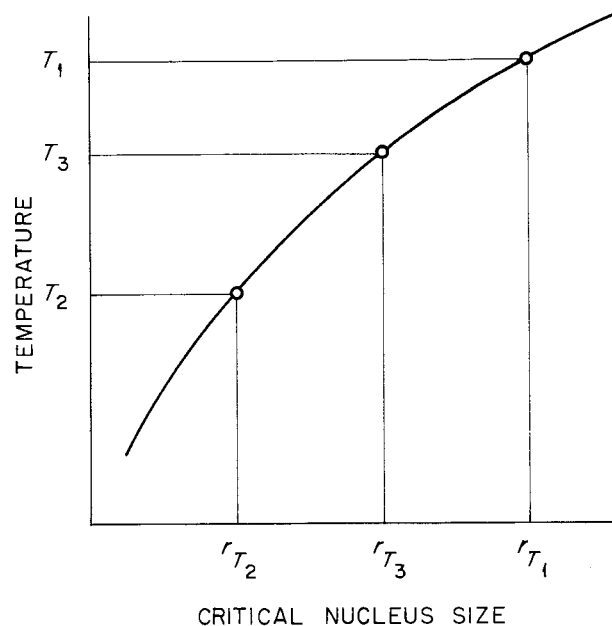


Fig. 6. Change of Critical Nucleus Size with Temperature (Schematic).

nuclei size distribution and by observing the change in physical properties when specimens are heated to various temperatures so that all nuclei smaller than the critical size are dispersed.

Possible assumptions are that precipitate particles in the range of sizes *A* (Fig. 7) effect an increase in resistivity and that particles in the range of sizes *B* effect an increase in hardness. A further assumption is that there is a pattern of nuclei established by irradiation or aging at a low temperature which may be described by some distribution function, *C*. If the critical size particle for stability at temperature *T* is represented by r_T , and if nucleated specimens are heated to temperature T_1 , then particles smaller than r_T will be dispersed with the result that they will no longer affect the physical properties. The change in physical property between the solution-quenched and nucleated conditions is represented by ΔP , the change in physical property when nuclei smaller than r_T are dispersed is represented by $\Delta P'$. For the hypothetical situation described by Fig. 7, the quantity $\Delta P'/\Delta P$ will be 1 if the nucleated specimen is heated to a temperature greater than T_1 and will be 0 for nucleated specimens heated to a temperature less than T_2 . Between these temperatures $\Delta P'/\Delta P$ will vary be-

tween 1 and 0. In this hypothetical case the variation of $\Delta H'/\Delta H$, the retrogression measured by hardness, will not coincide with $\Delta R'/\Delta R$, the retrogression measured by resistance. The particle sizes affecting these properties will thereby be resolved as shown schematically in Fig. 8.

If a retrogression behavior of the type shown in Fig. 8 were to be observed in copper-beryllium alloy, it would indicate that the resistivity increases during aging and irradiation are not due to lattice strain, since at T_3 the resistivity effects have been removed, whereas the absence of retrogression measured by hardness would indicate that most of the strain is still present in the lattice. Evidence has been presented⁽³⁾ previously that supports this theory. Nucleated specimens showed complete retrogression as measured by resistance at 300°C. At this same temperature no retrogression in hardness was observed. These experiments have been extended in order to obtain complete retrogression curves of the type shown in Fig. 8. The previously reported differences at 300°C were again observed, and complete retrogression of hardness was observed at 350°C. The

(3) W. E. Taylor, G. T. Murray, and F. M. Blacksher, "Subsequent Aging and Retrogression Phenomena in a Copper-Beryllium Alloy," *op. cit.*, ORNL-1214, p. 15.

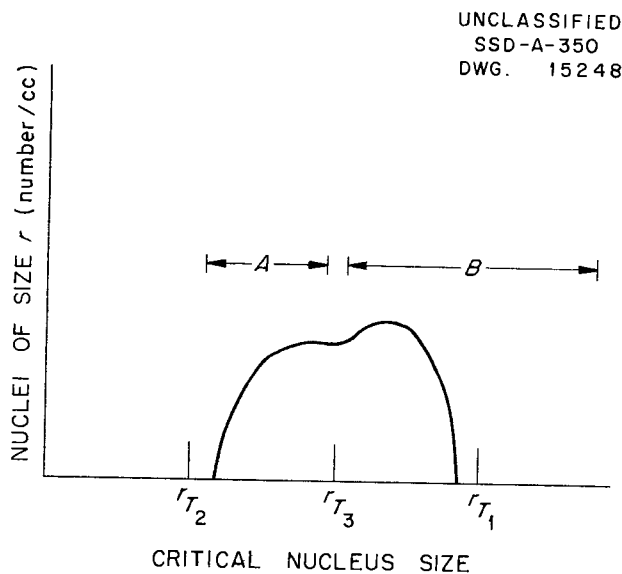


Fig. 7. Hypothetical Nucleated Condition Showing the Range of Size Affecting Resistance (*A*) and Hardness (*B*).

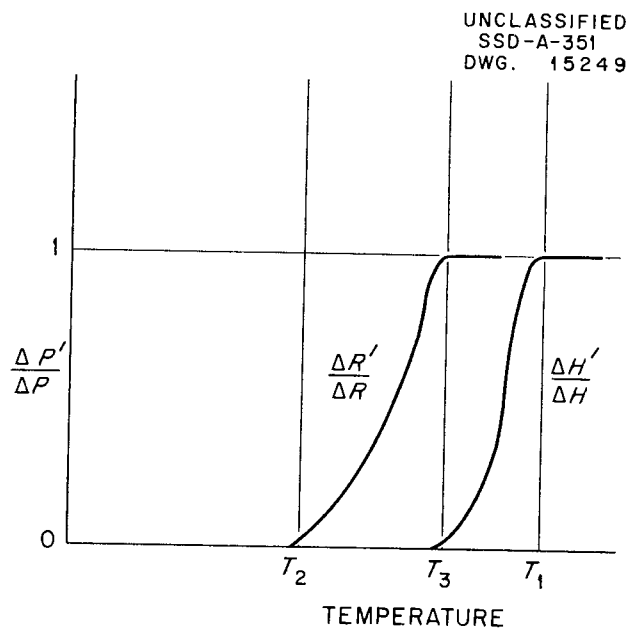


Fig. 8. Hypothetical Retrogression Curves Illustrating Resolution Between Particle Sizes.

SOLID STATE DIVISION QUARTERLY PROGRESS REPORT

data are not sufficiently reliable to determine the exact course of retrogression between these points, however, since the hardness measurements did not appear to be reproducible. The source of this difficulty is being investigated, and the experiment will be repeated.

The criticality of the nuclei stable at 300°C is also indicated by Fig. 9, where the maximum resistance increase observed at various temperatures is plotted against the aging temperature. The disappearance of the resistance increase at about 300°C indicates that the nuclei formed are no longer effective in increasing the resistance.

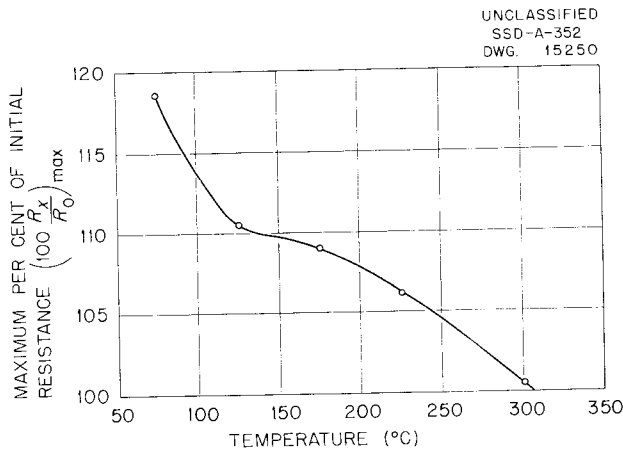


Fig. 9. Effect of Temperature on Maximum Resistance Increase During Aging of Copper-Beryllium Alloy.

EFFECT OF IRRADIATION ON SUBSEQUENT AGING OF COPPER-TITANIUM ALLOY

W. E. Taylor G. T. Murray

The investigation of the effect of irradiation on the subsequent aging of copper-titanium alloys has been extended to temperatures much lower than those previously reported.^(4,5,6) The aging curves (resistance) at 200 and 125°C are shown in Figs. 10 and 11. The rate of precipitation in the standard samples is extremely small at these temperatures compared with the rate at the higher temperatures. At these low temperatures it is again observed that the effect of irradiation is to decrease the subse-

quent rate of precipitation. The rate has been decreased to the extent that precipitation, as measured by the change in electrical resistance, has not commenced during the aging periods used in these experiments. However, this low-temperature aging has produced an effect on the irradiated specimens; on subsequent aging at a higher temperature (400°C) the irradiated specimens age at approximately the same rate as the standard specimens; the aging curves are shown in Figs. 12 and 13.

(4) W. E. Taylor, G. T. Murray, and F. M. Blacksher, "Radiation Effects in Supersaturated Solid Solutions, Physics of Solids Institute Quarterly Progress Report for Period Ending April 30, 1951, ORNL-1095, p. 51, esp. p. 60.

(5) W. E. Taylor, G. T. Murray, and F. M. Blacksher, "Neutron Irradiation of Age Hardening Alloys," *op. cit.*, ORNL-1128, p. 20, esp. p. 23.

(6) W. E. Taylor and G. T. Murray, "Effect of Irradiation on Subsequent Aging of a Copper-Titanium Alloy," *op. cit.*, ORNL-1214, p. 13.

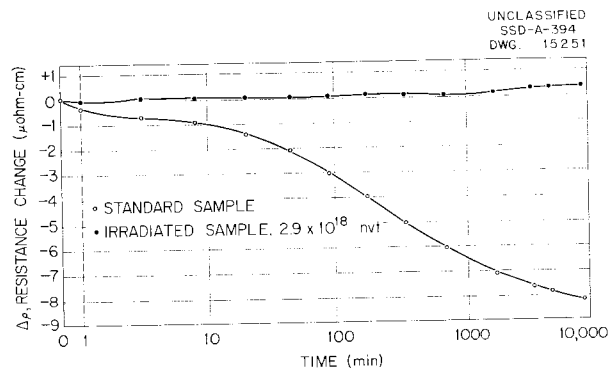


Fig. 10. Radiation Effect on Aging of Copper-Titanium Alloy at 200°C.

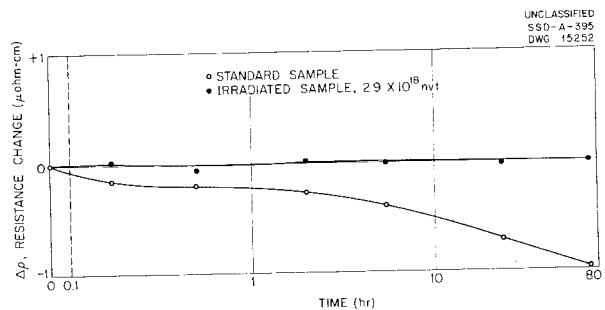


Fig. 11. Radiation Effect on Aging of Copper-Titanium Alloy at 125°C.

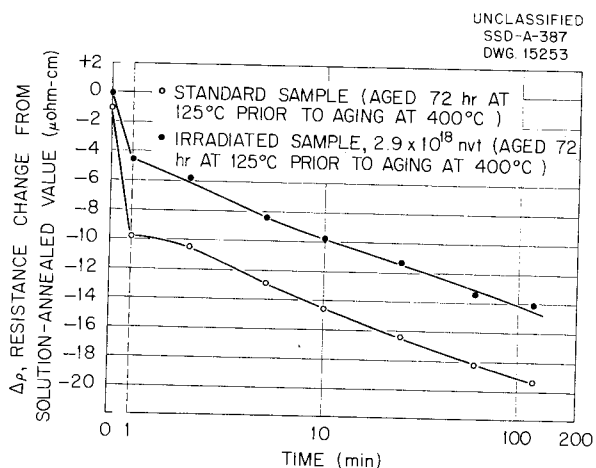


Fig. 12. Radiation Effect on Aging of Copper-Titanium Alloy at 400°C After Prior Aging at 125°C.

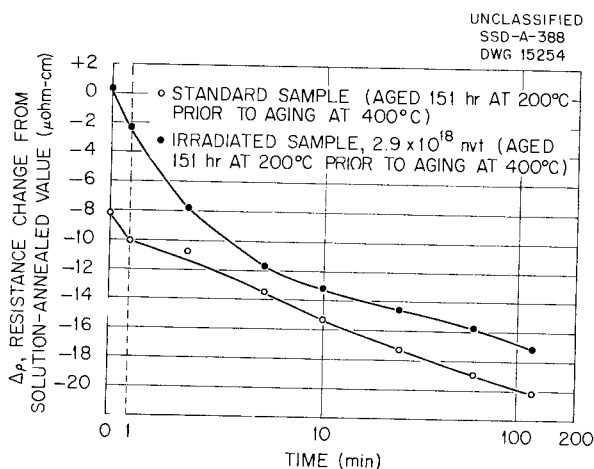


Fig. 13. Radiation Effect on Aging of Copper-Titanium Alloy at 400°C After Prior Aging at 200°C.

IRRADIATION OF SUPERSATURATED SOLID SOLUTIONS IN THE LITR

W. E. Taylor G. T. Murray
F. M. Blacksher

During the past quarter the LITR has become available for experiments on radiation effects in metals. This is a particular advantage, since the higher fluxes of the LITR allow exposures to integrated fluxes of much higher values in shorter

periods than those previously experienced in the X-10 graphite pile. However, at the present time, neither the flux nor the ambient temperature of the reactor is accurately known. A number of survey experiments are in progress. An investigation of the increase in the electrical resistance as a function of the integrated power of a copper-beryllium alloy has begun. The resistance has increased approximately 16% during an exposure of one month. Hardness and resistance specimens of copper-titanium and aluminum-silicon alloys have been irradiated for a 6-week period.

BETA PHASE COPPER-BERYLLIUM ALLOY

W. E. Taylor G. T. Murray

X-ray investigation of the structure of the beta phase copper-beryllium alloy previously reported⁽⁷⁾ has been continued in cooperation with the x-ray group of the Metallurgy Division. Rotating crystal and precession camera techniques have been used.

CREEP UNDER IRRADIATION

W. W. Davis J. C. Wilson
J. C. Zukas

Type-347 Stainless Steel Creep Tests. An extended cantilever creep test of a type-347 stainless steel at a series of temperatures from 1200 to 1400°F in the X-10 graphite pile under a stress of 8000 psi has been completed; the test lasted 950 hr. Secondary creep rates varied by a factor of 1200 over this temperature range, and a plot of reciprocal temperature vs. creep rate was linear except for the highest temperature point. Since duplicate bench tests under the same conditions are in their 400th hour, no comparison of inpile and bench data is yet available.

A 500-hr test was run on type-347 stainless steel at 1500°F and 1500 psi in the X-10 graphite pile without a strain-measuring microformer, since in 500 hr the creep strain would exceed the maximum microformer travel. The beam deflection was

(7) W. E. Taylor and G. T. Murray, "Investigation of a Beta Copper-Beryllium Alloy," *op. cit.*, ORNL-1214, p. 13.

SOLID STATE DIVISION QUARTERLY PROGRESS REPORT

measured with a cathetometer after the sample was withdrawn from the reactor. The strain in the bench test exceeded that of the inpile test by 5%, which is contrary to what would be expected from extrapolation of data reported earlier.⁽⁸⁾ This experiment will be repeated. Another test was run under the same conditions except for a shorter period, which allowed the use of an extensometer, and up to about 200 hr this specimen showed less creep than earlier specimens, but after that it appeared to go into third-stage creep. Interpretation of the results awaits examination of the apparatus to see if the test specimen might have been fabricated from a material other than type-347 stainless steel.

Nickel Creep Tests. A single inpile cantilever creep test was run on an electrolytic nickel sample at 1300 and 1250°F at a maximum fiber stress of 2000 psi. The material was annealed at 1500°F for 5 hr after a cold reduction of 40%. The temperature of 1300°F was chosen as the maximum temperature at which the grain structure was known to remain stable during the test. Figure 14 shows the data from both inpile and bench tests. In common with the earlier work on type-347 stainless steel,⁽⁸⁾ the curves show that the inpile strain vs. time curve becomes more nearly linear, shows less strain, but exhibits a higher creep rate than its bench counterpart at about 100 hr. This is seen more clearly in the plot of the creep rate vs. time in Fig. 15. At about 120 hr the inpile rig had reached an approximately constant strain rate, whereas the rate in the bench test was still decreasing.

During the first few hours after the temperature was reduced to 1250°F (after 146 hr at 1300°F) the rates of both tests were approximately equal. After 162 hr of the test period an extended unscheduled pile shutdown caused some confusion. From a time midway through the shutdown (after 180 hr of the test period) until the end of the test the rate of the inpile test remained about 25% below the bench test. Although part of this lower rate may have been caused by a slight drop (13°F) below the test temperature of one end of the speci-

men, the fact that the whole bar (instead of just one end) would have had to drop a corresponding amount to account for a 20% decrease in rate indicates that there was a real reduction of creep rate in the irradiated sample compared with the bench test. The creep rate of the bench test continued to be relatively constant ($\pm 3\%$) for the remainder of its 500-hr test period. Superficially, at least, it has been shown that radiation can cause an increase or decrease in the creep rate, depending on test conditions. Bench tests of the nickel were run at several temperatures and stresses to provide a guide to future work.

Inconel Creep Tests. Inpile and bench tests of inconel at 1500°F in the cantilever rig have begun. Pretreatment has consisted of a 2-hr anneal at 1650°F. Later tests are planned after a 2050°F anneal if grain size determinations now in progress show that grain growth is not so excessive that individual grains approach the specimen size. The creep strength of inconel at 1500°F is almost tripled after it is annealed at the higher temperature.

Apparatus Development. A furnace has been developed for the cantilever apparatus that will permit the test temperature to be extended to 1700°F without furnace burnouts.

The behavior of microformers (linear variable differential transformers or LVDT's) during changes in pile power has been given closer attention. Primary-to-secondary leakage resistance appears to account for most of the effect reported earlier,⁽⁹⁾ i.e., the microformer output voltage change with pile power. Leakage between the inpile leads (approximately 1000 megohms pile down, 100 megohms pile on) did not account for the anomaly, and even a 5-megohm resistor bridged between any two of the microformer terminals appearing at the pile face did not change the output voltage so much as did the variations in pile flux.

The results of a more recent test during a pile startup following a 1.5-hr shutdown are shown in Fig. 16. The period of observation was about 45 sec, and during this time the pile power was

⁽⁸⁾J. C. Wilson, R. A. Weeks, J. C. Zukas, and W. W. Davis, "Creep Under Irradiation," *op. cit.*, ORNL-1128, p. 29.

⁽⁹⁾J. C. Wilson, J. C. Zukas, and W. W. Davis, "Creep Under Irradiation," *op. cit.*, ORNL-1095, p. 46, esp. p. 50.

increased at a fairly uniform rate from a few hundred watts to 4 megawatts. The leakage resistance from primary to secondary dropped from 59 to 16 megohms, and the microformer output voltage decreased about 1 mv. When these curves were first plotted it appeared that there might be

some effect acting other than leakage resistance, since the rates of change of voltage and leakage resistance were different. It was noted, however, that the voltage change as a function of pile power was nearly linear rather than hyperbolic as was found earlier. Investigation of the input circuit of

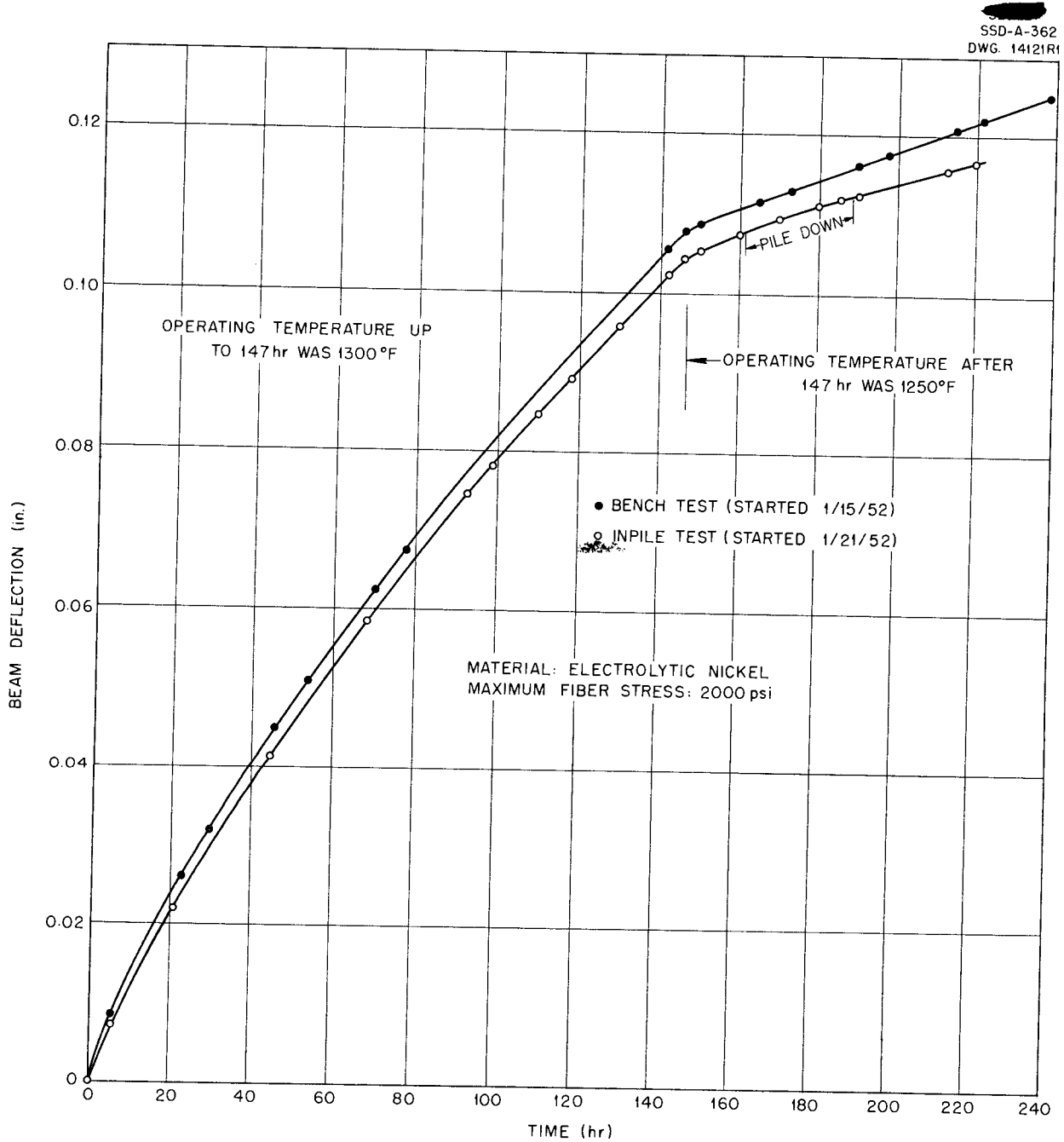


Fig. 14. Comparison of Bench and Inpile Creep Curves.

SOLID STATE DIVISION QUARTERLY PROGRESS REPORT

the megohmmeter that fed the recorders showed that it loaded the microformer circuit with a 10-megohm resistance, which in parallel with the true microformer leakage gave the resistance value plotted in the upper curve in Fig. 16. It can be seen that qualitatively at least, the observed microformer output voltage and the leakage resistance between the primary and secondary of the microformer change in the same manner. The megohmmeter has been modified to have a higher input impedance, so that the validity of the foregoing conclusion may be further verified.

There are several combinations of linkage of the primary and secondary by abnormal leakage resistance so that increases or decreases in output voltage, which depend on the construction of the microformer and the points in the windings between which the most leakage occurs, might be expected. The fact that in the earlier test, shunting a 5-megohm resistor across any combination of leads to the inpile microformer could not account for changes in output voltage of the magnitude caused by flux changes can be explained by assuming that leakage occurred between the inpile jumper connecting one end of each of the secondary windings.

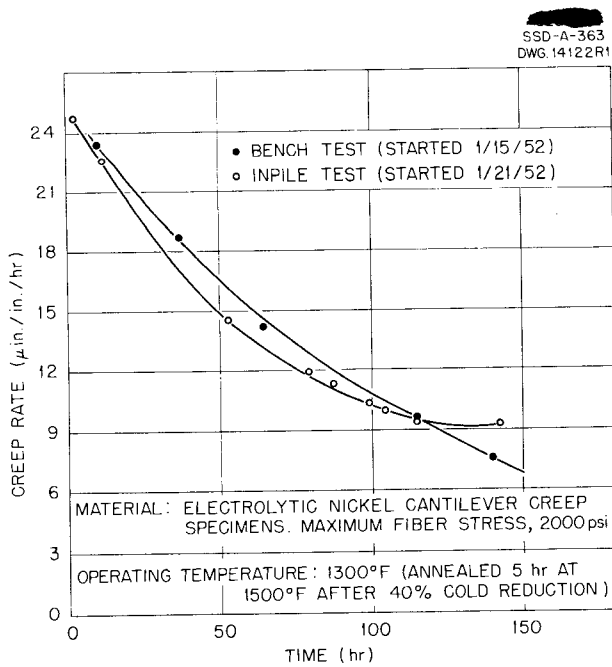


Fig. 15. Comparison of Bench and Inpile Creep Rates.

Since the jumpered connection is not brought out to the pile face, it was impossible to duplicate the previous conditions of leakage with an out-of-pile resistor. Future rigs will carry a connection to the jumper so that the foregoing supposition can be verified. It is suggested that the measurement of leakage resistance to ground,⁽¹⁰⁾ recommended as a criterion for indicating microformer breakdown under irradiation, be replaced or at least supplemented by a measurement of interwinding leakage as was done previously.

The melting points of the pure metals that are commonly employed for thermocouple calibration do not lie sufficiently close to 1500°F, the desired temperature for inpile calibration of thermocouples intended for use in the ANP creep tests. An investigation of sodium chloride (m. p. about 1480°F) for the purpose of calibrating couples has begun. A bench rig using 0.4 g of the salt in a quartz tube has been tested for about two weeks. The high heat of fusion of the salt (142 cal/g) gives marked arrests in the cooling curve. The stability of the salt in the quartz has been good so far, and a number of quartz vessels are being fabricated in the glass shop. The salt will be sealed under vacuum inside the vessel, and a tubular well extending upwards from the bottom will permit the thermocouple to reside effectively in the middle of the melt and yet be in any desired atmosphere. The whole apparatus will weigh less than 20 g, including the furnace and insulation.

Long-time stability of the sodium chloride in quartz will be investigated in an apparatus of larger size but of identical geometry by the use of a platinum-rhodium thermocouple calibrated against a thermocouple that has been calibrated by the Bureau of Standards. The mass of the system has been kept small so that gamma heating in the MTR will not be excessive. If sodium chloride proves unsuitable, the silver-copper eutectic or the minimum melting point composition of the copper-manganese alloy system will also be tried. A number of chromel-alumel couples have been tested in air for long periods at 1500°F and will be calibrated as soon as the calibrating furnace in

(10) L. A. Cook and W. E. Johnson, "In-Pile Test of Microformer," *Proceedings of the Irradiation Damage Conference at Westinghouse Atomic Power Division March 6 and 7, 1951*, TID-5021, Paper 9, p. 50.

the Instrument Department standards room is restored to service.

The dimensions of hole HB-3 in the LITR have been accurately measured, and the figures have been incorporated in the final design of the hole sleeve that is being built in the shops. A mockup

of the inner end of the hole facility has been completed and will be used to determine the cooling efficiency and the effect of coolant flow, reduction, or stoppage. It will also be used to test the experimental can-pressurizing and leak-detecting systems. Instrumentation for the latter system has been assembled.

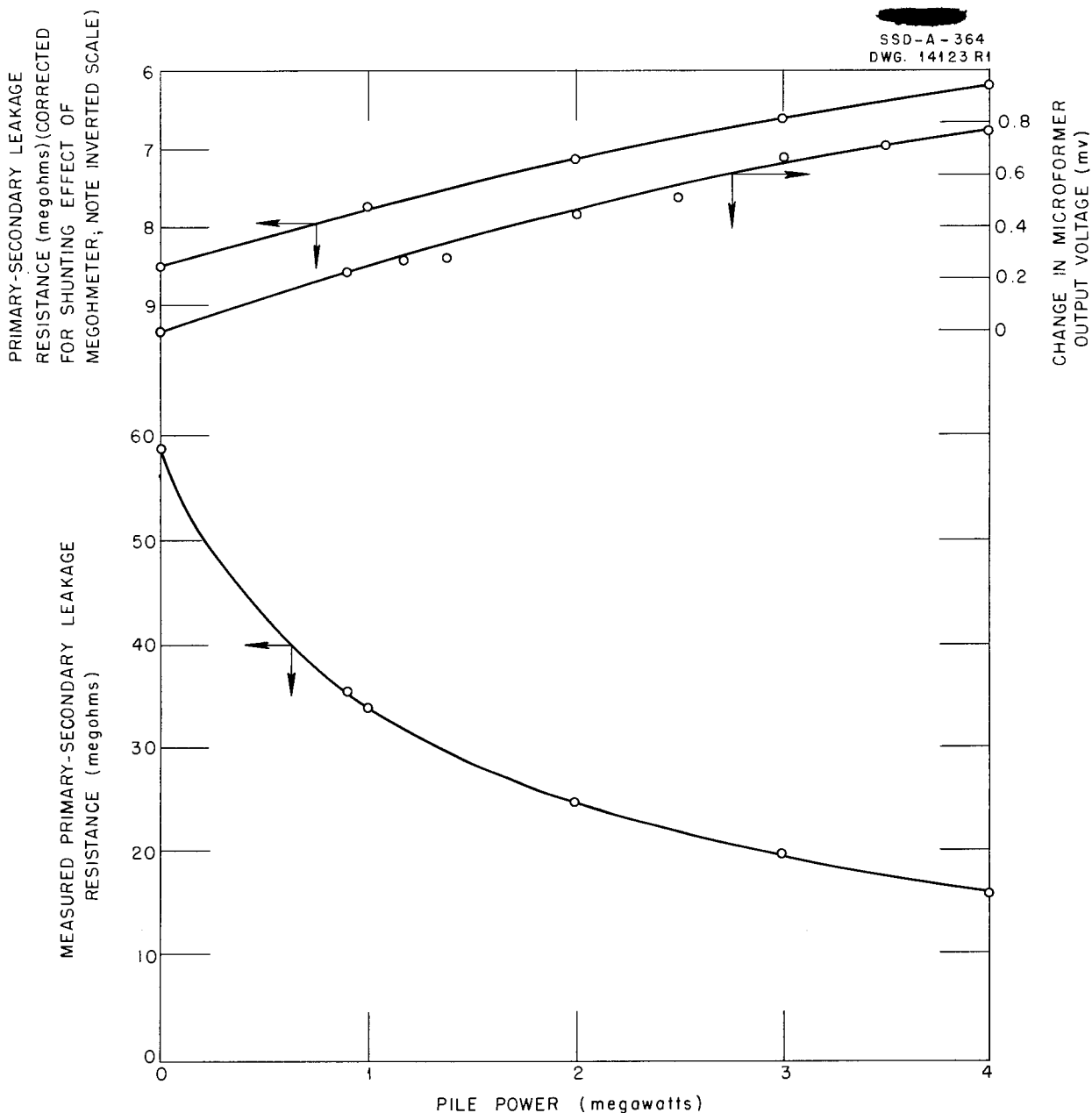


Fig. 16. Effect of Pile Power on Output Voltage and Leakage Resistance of Schaevitz Model 18-LCT Microformer.

SOLID STATE DIVISION QUARTERLY PROGRESS REPORT

A new type of extensometer, which will utilize a Bourdon tube distended by pressure from control instrumentation, is being considered for measuring creep strain. As the specimen extends, the tube will be pressurized at intervals until its free end contacts an element attached to the specimen. Contact will be indicated electronically by a device already constructed. It has been reported⁽¹¹⁾ that sensitivities of ~~2000~~ 4 $\mu\text{in.}$ are attainable in this manner, and experience at the Laboratory on commercial creep machines shows that considerably better than 25 $\mu\text{in.}$ sensitivity is easily attainable. The interest in the Bourdon tube has developed from its small mass (a 2-g tube has been fabricated for test), uniform geometry as far as heat loss characteristics are concerned, calibration dependence only on temperature that can readily be distributed uniformly, and elastic modulus, which in most metals is insensitive to virtually all conditions except temperature. Also, by varying the tube size and radius the range of travel may be varied from a few thousandths of an inch to more than a quarter of an inch with comparable percentage accuracy over any range. As a result it may be tailored to the requirements of any individual test.

Several preliminary mechanical designs for the MTR apparatus assembly have been evolved. The basic differences are in the means of stressing the specimen. Either gas pressure acting on a bellows or a dead-weight load with a force-multiplying lever arm system will be used. The bellows system is not usable at low load because of the large spring rate correction required, even with the very light bellows that have been procured, and the lever arm system is limited by cooling considerations in the loading weight. As planned, the weight will receive some gamma shielding by being located as far as possible from the active lattice and behind several inches of graphite and water. Tubular specimens are favored because calculations have shown that even with solid specimens as small as 1/8 in. in diameter the center may be several degrees higher in temperature than the outside.

⁽¹¹⁾M. I. Hetényi, *Handbook of Experimental Stress Analysis*, p. 672, Wiley, New York, 1950.

RADIATION DAMAGE TO FERROMAGNETIC MATERIALS

R. A. Weeks

As a further aid in the determination of microformer inpile reliability, a study of the effect of irradiation on the value of the initial permeability of several ferromagnetic materials is being conducted. It should be possible to determine qualitatively whether materials with a high initial permeability are affected more or less than those with low initial permeability. This kind of measurement is particularly attractive, since the core of the microformer is usually in a field that does not exceed 10% of its saturation value. Hence, if the change in output is due to changes in the magnetic characteristics of the core, it seems reasonable to assume that the initial permeability is being affected in some way. Several specimens of magnetic materials have been obtained from the Arnold Engineering Company for a preliminary investigation. The specimens include Supermalloy with an initial permeability $\mu_0 = 78,000$, 4-79 M-Permalloy with $\mu_0 = 14,500$, and Deltamax with $\mu_0 = 560$. The effect of neutron irradiation on these values will be investigated. In addition to a study of the effect of irradiation on μ_0 , it is hoped that some study of the effect of irradiation on remanence and coercive force can be made. It may then be possible to select a core material that will be unaffected by irradiation.

AN EVALUATION OF TEMPERATURE CONTROLLERS

R. A. Weeks

J. C. Wilson

Developmental work on the tensile creep rig for the MTR has included an investigation of the characteristics of the Leeds and Northrup Speedomax Air Controller and PAT units for controlling the specimen temperature. These controllers were hooked up to control a quartz tube furnace containing a 0.01-in.-wall 0.1-in.-OD dummy specimen (see Fig. 17). In order to simulate gamma heating within the specimen, an on-off heating element was installed inside the dummy specimen. Power

UNCLASSIFIED
SSD - A - 408
DWG. 15255

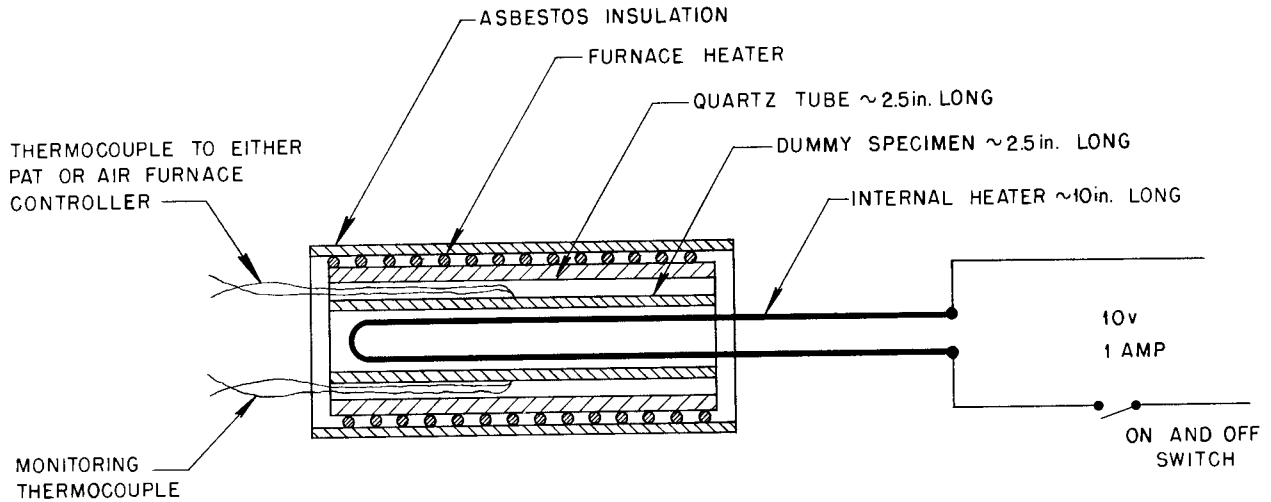


Fig. 17. System Used in Testing Controllers (Schematic).

to the internal heater was supplied at 2 watts per inch of specimen (5 w total). The on-off method of adding energy to the specimen is a more rigorous condition than is expected in the MTR experiments. When the internal heater is turned on or off, the air controller allows a maximum excursion of temperature of $\pm 7^\circ\text{F}$ and the PAT allows $\pm 6^\circ\text{F}$ (see Fig. 18). Either controller requires approximately 1 1/2 min to return the temperature to the control point under these conditions. The long-term stability of the controllers is now being tested.

RADIATION DAMAGE TO DIELECTRICS

R. A. Weeks

An investigation of the effects of neutron and gamma radiation on the electrical characteristics of various cables is planned. Measurements on the attenuation characteristics of the cables at 1000, 3000, and 8600 megacycles will be made during irradiation. Cables will be irradiated in the Bulk Shielding Reactor at a thermal-neutron flux level of approximately 10^9 neutrons/cm².sec. The period of exposure will be determined by the rate

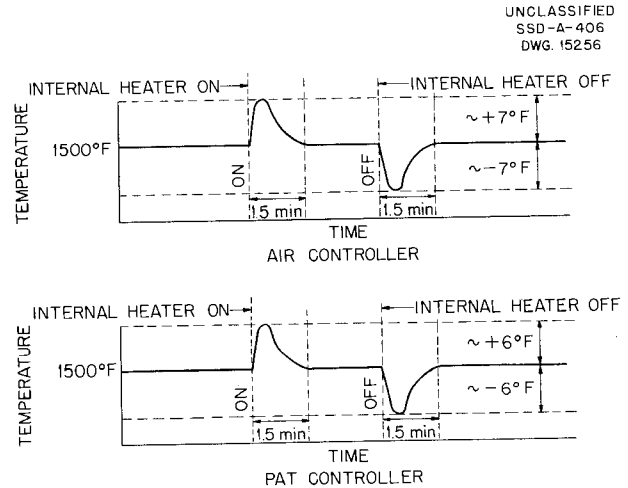


Fig. 18. Optimum Performance of Air and PAT Controllers.

of change of the attenuation. The total period of exposure will usually be no longer than two or three months.

Samples of the dielectric material will be obtained from the same batch as that used in the cable specimens. The sample material will be

SOLID STATE DIVISION QUARTERLY PROGRESS REPORT

formed into convenient shapes for measurements of loss tangent and attenuation⁽¹²⁾ before and after irradiation. Study will also be made of the effect of gamma irradiation only on the dielectrics.

These studies are also of interest to the Bureau of Ships in their selection of high-frequency cables for use in the vicinity of the Naval Reactor. They have agreed to supply much of the equipment and material to be used and to furnish occasional technical aid. The first of the dielectrics are to be received by ORNL in April.

IMPACT TESTS ON IRRADIATED STEEL

R. G. Berggren R. H. Kernohan

The impact tests on irradiated steel are the first in the study of the effects of radiation on materials of interest to the HRP.

While the homogeneous reactor radiation studies project was still in the planning stage, ANL reported decreases in impact resistance of nick-bend specimens as a result of irradiation at HEW.⁽¹³⁾ Several other low-carbon steels showed the same decrease in impact strength.^(14,15,16) ANL contacted the Solid State Division in the hope that additional information could be obtained.

Since a significant change in impact strength would seriously affect the design of pressure vessels and other construction materials used in homogeneous reactors, it was decided to place immediate emphasis on this problem. Among the Solid State Division's irradiated materials there were three tensile test specimens of ASTM type

(12) S. Roberts and A. von Hippel, "A New Method for Measuring Dielectric Constant and Loss in the Range of Centimeter Waves," *J. Applied Phys.* 17, 610 (1946).

(13) W. F. Murphy to S. H. Paine, Jr., *Naval Reactor Materials Testing Division Program M-9, Group 2*, Argonne National Laboratory Memorandum ANL-FF-100z (July 13, 1951).

(14) W. F. Murphy to S. H. Paine, Jr., *Naval Reactor Materials Testing Division Program M-3 - Post Irradiation*, Argonne National Laboratory Memorandum ANL-FF-100ac (Aug. 15, 1951).

(15) W. F. Murphy to S. H. Paine, Jr., *Naval Reactor Materials Testing Division Program M-7, Group 9-B*, Argonne National Laboratory Memorandum ANL-FF-100af (Aug. 17, 1951).

(16) G. J. Deily to S. H. Paine, Jr., *Modified Izod Impact Tests - NRD Materials Testing Division Program M-15*, Argonne National Laboratory Memorandum ANL-FF-100an (Dec. 6, 1951).

A-70 steel. The specimens had been exposed to 7.5×10^{19} nvt at HEW in 1948. There were five identical unirradiated control specimens. All of these specimens were machined into substandard-size, round Izod bars, 0.178 in. in diameter by 5 3/8 in. in length, each having five circumferential notches 0.020 in. deep with a 0.005-in. radius at the root. The specimens were broken at each notch at controlled temperatures ranging from -112 to +302°F.^(17,18) Examination of the graph of impact strength vs. temperature (Fig. 19) shows a pronounced elevation of the impact transition temperature in the case of the irradiated specimens. The "ductile" impact strength of the irradiated specimens is nearly half that for the unirradiated control samples, although no truly ductile fracture occurred for the irradiated specimens, whereas there were 13 ductile fractures in the control tests.

Several metals of direct interest to the HRP have been chosen for further testing after discussions with E. C. Miller of the Metallurgy Division. Specimens of SAE-1040 steel are being prepared for irradiation in hole No. 1867 of the X-10 graphite pile. Type-304 ELC stainless steel and other metals will be irradiated as soon as possible.

(17) K. F. Smith and D. O. Leeser to H. Etherington, *Impact Tests on Irradiated Steel at Oak Ridge*, Argonne National Laboratory Memorandum ANL-HE-1225 (Jan. 25, 1952).

(18) The writers wish to thank K. F. Smith and W. K. Anderson of Argonne National Laboratory for their cooperation in this investigation.

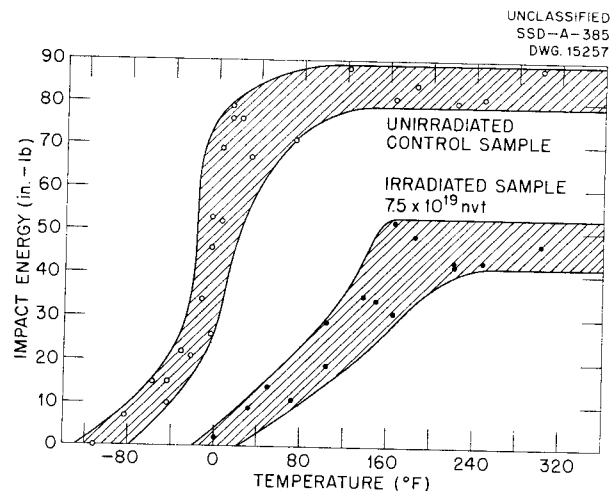


Fig. 19. Impact Strength of Irradiated ASTM Type A-70 Steel.

ENGINEERING PROPERTIES

X-10 GRAPHITE PILE LIQUID-METALS LOOP

C. D. Baumann	D. T. James
R. M. Carroll	M. T. Morgan
C. Ellis	O. Sisman
W. W. Parkinson	

An inconel loop containing sodium⁽¹⁾ was operated in the X-10 graphite pile for two weeks. The first loop,⁽²⁾ which was heated by three 4000-w 230-v Calrod elements in series, failed because of arcing of the heaters during the bench test. A similar loop was constructed with two sets of Calrod tubular heaters connected in parallel. Each set of heaters was made up of three 4000-w, 230-v Calrod elements connected in series. By operating the two heaters in parallel it was possible to reduce the voltage from 720 to 440 and thus increase their life.

This loop was bench tested successfully and was operated in the X-10 graphite pile for a period of two weeks. During the latter part of each week the rate of flow of sodium through the loop gradually decreased until flow ceased, in spite of increased power to the electromagnetic pump. Flow was restored after the first stoppage by alternately pressurizing and evacuating the system, but circulation could not be started after the second stoppage and operation of the loop was halted. Circulation was maintained in the loop for 115 hr at 1500°F and 50 hr at 1000°F while the pile was in operation. Flow was adjusted to maintain a temperature of 1100°F at the pump cell when the inpile loop temperature was 1500°F. This flow was about 1 ft/sec. During each stoppage radioactive decay curves were obtained for a part of the loop outside the pile. These curves are being examined for evidence of long half-life corrosion products from the inconel tube walls.

(1) C. D. Baumann, R. M. Carroll, and O. Sisman, "Liquid-Metal Loops," *Physics of Solids Institute Quarterly Progress Report for Period Ending April 30, 1951*, ORNL-1095, p. 69.

(2) C. D. Baumann, R. M. Carroll, O. Sisman, W. W. Parkinson, and C. Ellis, "X-10 Graphite Pile Liquid-Metals Loop," *Physics of Solids Institute Quarterly Progress Report for Period Ending October 31, 1951*, ORNL-1214, p. 35.

The loop has been partly withdrawn from the pile, and the inactive portion has been removed entirely. After the active portion of the loop has decayed sufficiently, it will also be removed and another loop now being assembled will be inserted. Although an accurate determination of the cause of flow stoppage in the loop cannot be made until the activity drops to levels safe for handling the materials, several design changes are being incorporated in the new loop to eliminate possible causes of stoppage.

LIQUID-METALS STRESS-CORROSION LOOP

W. E. Brundage	A. S. Olson
R. M. Carroll	O. Sisman
C. Ellis	W. W. Parkinson

Shielding will be simplified for experiments that are performed at the flux levels of the LITR if all parts of the system through which sodium flows can be kept within the hole in the reactor shield. The design of a loop, a pump, and a creep and corrosion specimen, all of which can be enclosed by the reactor shield, has been completed. This apparatus has been described in the previous quarterly report,⁽³⁾ and the details of operation have been discussed along with the operating characteristics of a water-circulating, glass mockup pump.

Fabrication of the loop, pump, and associated equipment in the Research and Central Shops is about 80% complete. The shops were unable to fabricate a sodium pump tank that was leak-tight, as was specified in the original design. A tank of revised design is under construction, and assembly of various parts of the auxiliary equipment has been started. The design of instrumentation has been completed, including the alarm and pile interlock circuits. The construction of the instrument panel board has been completed, and all necessary instruments have been procured. A

(3) A. S. Olson, W. E. Brundage, W. W. Parkinson, and O. Sisman, "LITR Liquid-Metals Loop," *op. cit.*, ORNL-1214, p. 32.

SOLID STATE DIVISION QUARTERLY PROGRESS REPORT

preliminary presentation of the equipment and the instrumentation has been made to the Reactor Experiment Review Committee.

Heater units to enclose the specimen and the loop have been received, but these units have a power rating of 2150 w, rather than 5000 w as was specified originally. It was found that the available space limited the heater power to the lower figure. In addition, heater cores for the center space of the sodium tank assembly have been received. These units, wound in longitudinal slots with No. 28 Nichrome V wire, will provide an additional 2000 watts.

As described earlier,⁽³⁾ the pump and loop system will be enclosed in a helium atmosphere. To minimize the danger of oxidation at the 1500°F operating temperature, a helium purifier has been designed that should reduce the oxygen content to 8 ppm and the water to 1 ppm or less. The purifier consists of a stainless steel scrubber tower, 4 ft high and 3 in. in diameter, and associated traps and filters. The tower will contain sodium-potassium eutectic, which is liquid at room temperature.

The pneumatic extensometer (an orifice varied by a movable needle) discussed in the previous quarterly report,⁽³⁾ has been fabricated of inconel and is now being calibrated. The conical shape of the point of the movable needle has been altered in such a way that the gaging pressure is quite linear over the range of 0.010 inch. A satisfactory adjustable leak valve could not be obtained for use as the first or fixed orifice. This orifice must present a fixed aperture, except to provide a high and low range for the instrument. To satisfy these conditions, this orifice is being assembled from interchangeable drilled orifice plates.

A glass pump-and-loop system circulating water has been operated⁽³⁾ to test the performance of the pump and its associated controls. To determine the suitability of the pumping method for sodium, the stainless steel bench model of the LITR system was connected to the instruments and pressurizing controls constructed for the glass system. The pressure controlling and recording apparatus was modified by elimination of the

amplifying air relay and replacement of the two pressure cells by a single cell and a differential pressure transmitter. The system was filled with a measured amount of sodium that had been filtered through a 5- μ "micrometallic" stainless steel filter while under a dry helium atmosphere, and the pump was operated in the same manner as that described for the water system in the last quarterly. The rate of flow of sodium circulated through the loop was recorded directly from an electromagnetic flowmeter incorporated in the loop, and a relation was determined for the differential pressure in the two halves of the pump tank as recorded from the transmitter and pressure cell by a Speedomax. It is necessary to have such a flow measuring device since it is not possible to use the electromagnetic flowmeter inside the pile. The loop and pump system has operated for short intervals at 1000°F, and this temperature is being raised to investigate check-valve operation and vapor condensation problems for extended periods of operation at 1500°F.

MTR FLUORIDE-FUEL LOOP

W. W. Parkinson

O. Sisman

A dynamic corrosion experiment is planned for the MTR. The first liquid to be tested in the MTR in-pile loop will be the fused fluoride fuel that is being developed for the aircraft reactor. Equipment and procedures for this experiment were discussed with Phillips Petroleum personnel at the MTR site in December.

Fuels containing 6 to 10 wt % U^{235} will produce about 2000 w/cc at MTR fluxes. It will be necessary to have an intermediate heat exchanger to keep the fuel temperature down to 1500°F with this heat flux. Because of this added complication, it is most likely that the first MTR experiment will be a simple loop containing no stressed section. It is thought, however, that it may be possible to obtain some heat transfer data on this system⁽⁴⁾ and perhaps also some data on the accumulation of fission xenon from such a system.

⁽⁴⁾This work will be done in cooperation with H. F. Poppendick.

PHYSICAL PROPERTIES OF IRRADIATED PLASTICS AND ELASTOMERS

C. D. Bopp R. L. Towns
O. Sisman W. K. Kirkland

In the study of the nature of the radiation-induced changes in plastics and elastomers it is useful to know whether gas is evolved. Hydrogen is the largest gaseous constituent for many organic materials.⁽⁵⁾ When hydrogen-containing plastics or elastomers are used in shielding fast neutrons, it is important to know how long the hydrogen content of these materials will be retained.

Preliminary determinations of the volume of gas evolved by irradiated plastics and elastomers are listed in Table 1. From 0.2 to 0.5 g of sample material was sealed in a glass capsule of about 3-cc volume. The capsules were irradiated in water-cooled hole 19 of the X-10 graphite pile. Three weeks after removal from the reactor the capsules were broken open, and the volume of gas evolved was measured over mercury.

All of the plastics that give off no gas for the longest irradiation period listed (4.6×10^{18} nvt) show no change in physical properties⁽⁶⁾ for periods of irradiation up to 10^{19} nvt, with the exception of Styron 475. Styron 475 is a modified polystyrene plastic that decreases in impact strength upon irradiation until it is similar to unmodified polystyrene. The plastics that give off only a small amount (1 to 3 cc) of gas at 4.6×10^{18} nvt change only slightly in physical properties. However, some of the elastomers give off no gas at 2×10^{18} nvt, although they show pronounced changes in their physical properties. Nylon and polyethylene give off gas, which indicates that the irradiation-induced hardening of these materials is accompanied by a change in chemical composition.

A second batch of elastomers, which have been compounded at the B. F. Goodrich Research Center,

(5) R. O. Bolt and J. G. Carroll, *The Effects of Fission Radiations on Lubricants and Lubrications; Final Report Covering Period January 26, 1948 to April 30, 1951*, NEPA-1844.

(6) O. Sisman and C. D. Bopp, *Physical Properties of Irradiated Plastics*, ORNL-928 (June 29, 1951).

will be tested for radiation stability. The first batch consisted of gasket compositions of commercially used elastomers.^(7,8) Compositions of the second batch of elastomers are given in Table 2.

Compound No. 1 is loaded with a large amount of asbestos filler. Mineral-filled plastics are radiation resistant;⁽⁶⁾ however, these materials are hard and rigid. Tests on compound No. 1 are intended to show whether the addition of a large proportion of a mineral filler will increase the radiation resistance of an elastomer.

Protective agents will be defined here as chemicals that increase the radiation resistance of the material "protected." In compounds Nos. 2 and 8, dodecyl mercaptan is included to determine whether this material will function as a protective agent. An oxygen-type cure was used for compound No. 8 since dodecyl mercaptan interferes with the sulfur cure that is generally employed. Dibutyl tin dilaurate is included as a protective agent in compound No. 3.

Butyl rubber softens under irradiation, while natural rubber hardens. To what extent these changes counterbalance each other in mixtures of the two will be determined for compounds Nos. 4, 5, 6, and 7.

Elastomers that were compounded for use as gasketing materials⁽⁷⁾ were placed in a constant strain compression jig (Fig. 20) and irradiated in water-cooled hole 19 in the X-10 graphite pile. The elastomers were removed from the jig, and the deformation was measured 30 min later.

A similar experiment was conducted in which the elastomers were placed in the jig for the same length of time but not irradiated. The specimens were cylindrical and were initially 1/2 in. thick and 1/2 in. in diameter; they were compressed in the jig to 3/8 in. in thickness. The maximum

(7) O. Sisman, R. L. Towns, C. D. Bopp, and W. K. Kirkland, "Physical Properties of Plastics," *op. cit.*, ORNL-1095, p. 75.

(8) O. Sisman, C. D. Bopp, W. K. Kirkland, and R. L. Towns, "Physical Properties of Irradiated Elastomers," *Physics of Solids Institute Quarterly Progress Report for Period Ending July 31, 1951*, ORNL-1128, p. 41.

SOLID STATE DIVISION QUARTERLY PROGRESS REPORT

Table 1

VOLUME OF GAS EVOLVED BY IRRADIATED PLASTICS AND ELASTOMERS

Determinations made at 25°C, 760 mm

Material	Gas Evolved (cc/g)				
	0.24×10^{18} nvt	0.47×10^{18} nvt	0.57×10^{18} nvt	2.0×10^{18} nvt	4.6×10^{18} nvt
Methyl methacrylate polymer	0	2	5	30	
Amino resins					
Aniline formaldehyde polymer					1
Melamine formaldehyde polymer (cellulosic filler)	0.3	0.3	1	6	19
Urea formaldehyde polymer (cellulosic filler)	0	2	4	12	
Casein plastic			0		12
Cellulosics					
Cellulose acetate			0.3		32
Cellulose acetate butyrate	2	3	4	25	
Cellulose propionate	1	5	7	27	
Cellulose nitrate	4	16	20	94	
Ethyl cellulose	0.4	6	7	22	
Polyethylene			0		116
Furane resin (asbestos and carbon filler)					0
Nylon FM-3003	0	3	6	19	
Phenolics					
Mineral filler					
Asbestos-fabric					0
Asbestos-fiber					0
Haveg 41					0
Cellulosic filler					
Paper-base			0		36
Paper-laminated		0	3	10	
Linen-fabric		2	2	6	
Polyester resins					
Allyl diglycol carbonate polymer	5	10	11	41	
Plaskon alkyd			0.3		3
Selectron 5038			0.1	3	
Styrene polymers					
Styron 411C					0
Styron 475					0
Vinyl-vinylidene chloride polymer			0.6		124
Elastomers					
5 Natural rubber			0	2	
6 Neoprene W			0	0	
3 Hycar OR-15			0	3	
1 GR-I 50	0		2	10	
2 GR-S 50				0	
4 Hycar PA-21	2		6	20	
8 Thiokol ST			0	2	
7 Silastic 7-170	0.5		3	14	

UNCLASSIFIED
DWG. 15258

deformation occurs when the specimen does not recover when it is removed from the jig and equals

$$\frac{1/2 - 3/8}{1/2} \times 100 = 25\%$$

In Table 3 the elastomers are ranked in order of least deformation, and results are listed for two irradiations. The lesser exposure of 0.03×10^{18} nvt is sufficient to decrease the elongation of the elastomers from 5 to 40% and to slightly increase the hardness of most of the elastomers.⁽⁸⁾ The values of deformation listed in Table 3 indicate that this compression set test is more sensitive to irradiation than changes of either of the other properties.

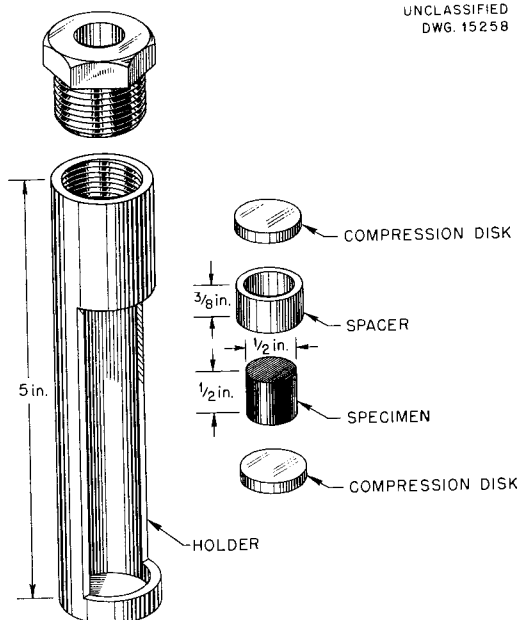


Fig. 20. Compression Jig.

Table 2

COMPOSITION OF SECOND GROUP OF IRRADIATED ELASTOMERS

Material	Content (parts by weight)							
	Elastomer No.							
	1	2	3	4	5	6	7	8
Natural rubber	100		100	50	25	10	100	100
Zinc oxide	5	5	5	5	5	5	5	5
Stearic acid	1	0.5	1	2	2	2	2	1
Phenyl naphthylamine	1	2	1	1	1	1	1	1
Captax	0.6		0.6	0.75	0.75	0.75	0.7	
Sulfur	3		3	2.5	2	1.5	2.5	
SRF black		40	70	70	70	70	70	70
Diphenyl guanidine				0.2	0.3	0.5	0.2	
Butyl rubber				50	75	90		
Calcium silicate				10	10	10		
Dodecyl mercaptan		10						10
Asbestos fiber	250							
Neoprene W		100						
Magnesium oxide		2						
Accelerator		0.5						
Dibutyl tin dilaurate			10					
Butyl rubber reclaim							60	
Lead oxide								10
Chloranil								5
Total	360.6	160	190.6	191.45	191.05	190.75	241.40	202

SOLID STATE DIVISION QUARTERLY PROGRESS REPORT

Table 3

EFFECT OF IRRADIATION ON THICKNESS OF ELASTOMERS UNDER COMPRESSION

Elastomer	Thickness Decrease (%)			
	In Jig 190 hr		In Jig 840 hr	
	Unirradiated	Irradiated 0.03×10^{18} nvt for 7.5 hr	Unirradiated	Irradiated 0.16×10^{18} nvt for 40 hr
Hycar OR-15	1.9	9.6	2.4	19.1
GR-S 50	2.4	11.7	3.1	19.5
Natural rubber	1.8	11.9	2.6	18.8
Hycar PA-21	1.9	10.5	2.2	21.5
Neoprene W	9.5	16.8	14.5	22.1
Silastic 7-170	0.8	18.2	1.3	25
Butyl (GR-I 50)	2.2	19.2	2.9	Tarry-fluid
Thiakol ST	2.5	24.6	4.5	25

PILE-INDUCED RADIATION IN MATERIALS OF CONSTRUCTION

C. D. Bopp R. L. Towns
W. K. Kirkland

The work on pile-induced radiation is continuing, and a topical report will probably be completed during the next quarter. No new materials have been added to this project during the past three months.

MEASUREMENT OF NEUTRON ENERGY SPECTRA

J. B. Trice

The measurement of neutron spectra used and the results from radiation damage experiments permit a better understanding of the fundamental relationship between energies of bombarding neutrons and the characteristics of the damage produced. An opportunity is afforded to correlate damage expected with damage measured, and therefore to predict on the basis of neutron flux measurements what will happen to a test material when it is

placed in a new position in the same reactor or in a different reactor.

The first phase of this project, the measurement of the energy spectrum of neutrons near a fuel element in the LITR, has been completed. The center of the upper pneumatic rabbit tube was chosen for this initial test because of (1) accessibility, necessary where fast sample removal is required, and (2) proximity to HB-1 and HB-6, horizontal beam holes to be used for radiation damage studies. Samples exposed in the high-energy neutron field were located at the center-north-lower edge of the reactor lattice. This location was 5.4 in. from uranium metal and separated from it by a beryllium piece. With respect to HB-1 and HB-6, it was about midway between their intersections with the reactor lattice (Fig. 21).

The method employed was essentially that described in ORNL-525.⁽⁹⁾ The high-energy range of the spectrum from approximately 2 to 6 Mev was measured with five threshold reactions for high-energy neutrons. The energy region from 100 to

⁽⁹⁾C. D. Bopp and O. Sisman, *The Neutron Flux Spectrum and Fast and Epithermal Flux in Hole 19 of the ORNL Reactor*, ORNL-525 (July 28, 1950).

UNCLASSIFIED
SSD - A - 393
DWG. 15259

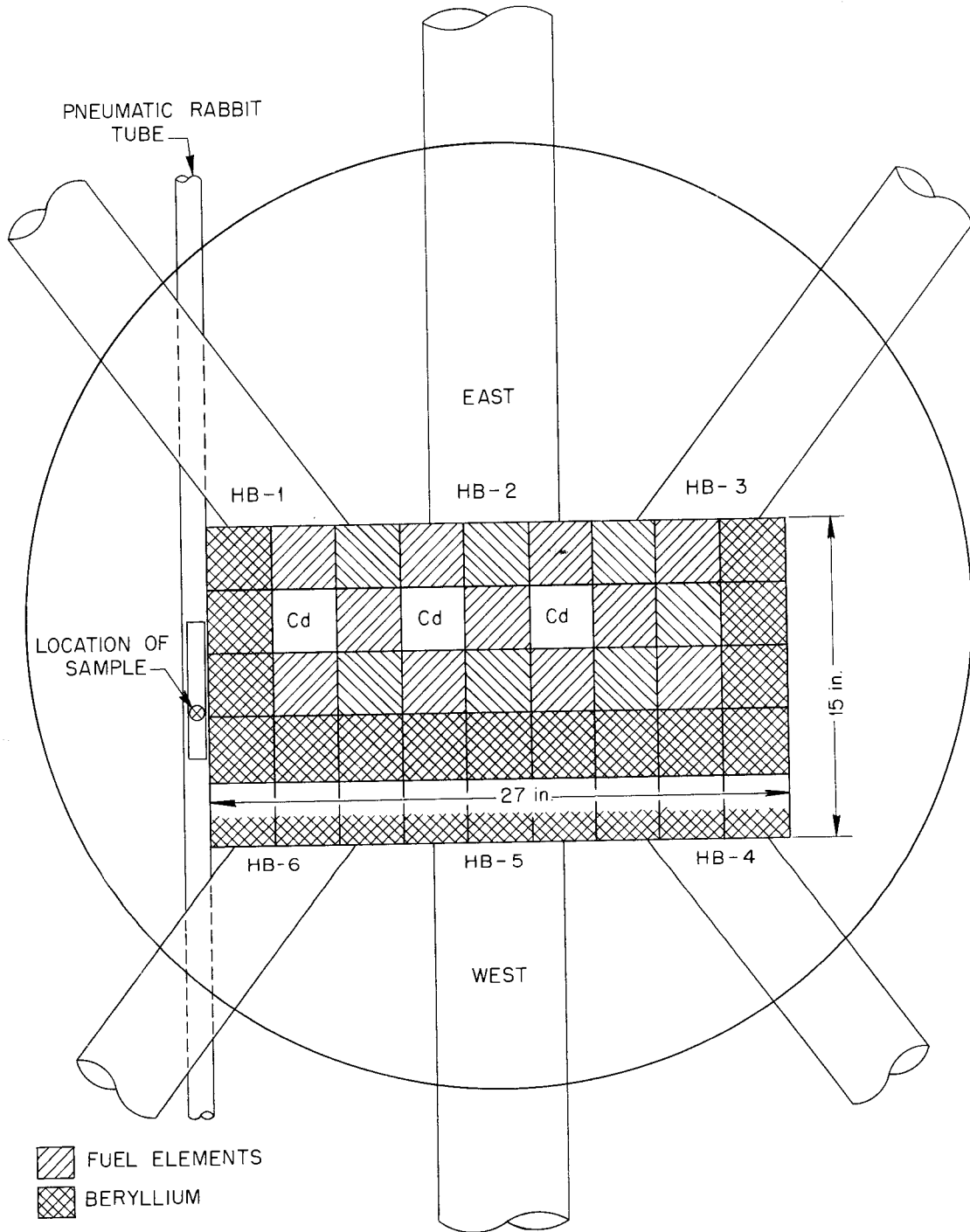


Fig. 21. Top View of LITR (Schematic).

SOLID STATE DIVISION QUARTERLY PROGRESS REPORT

10,000 ev was measured with five resonance reactions. In the thermal region the flux was measured with cobalt and corrected for temperature. In order to obtain some information about the spectrum in this region (0.025 to 1.0 ev), the thermal flux was expressed as a Maxwellian distribution, and the measured epithermal region that varies as $1/E$ was extended downward from the region of several electron volts until it intersected the high-energy tail of the Maxwellian curve. This intersection occurred at 0.2 ev where, according to a Maxwellian distribution, the neutron population is small. This was interpreted to mean that the $1/E$ part of the neutron spectrum begins here since the relative effect of thermals is very small above this energy. Recent preliminary experiments by the Physics Division with the neutron velocity selector near the position of these measurements indicate a $1/E$ epithermal spectrum starting between 0.2 and 0.3 ev.

The neutron spectrum in the LITR pneumatic rabbit tube is shown in Fig. 22. The high-energy

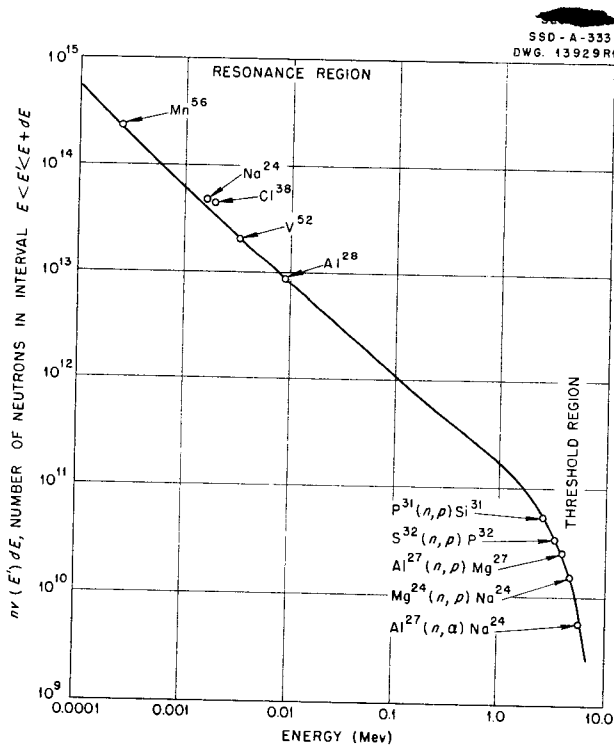


Fig. 22. Neutron Energy Spectrum in LITR Pneumatic Rabbit Tube (North Lower Center Reactor Lattice).

region agrees essentially with the fission spectrum from 3 to 7 Mev. The ratio in the LITR of total integrated flux above thermal energies (cadmium cut off) to total thermal flux at the same position is 0.31. This is less than the same ratio, 0.55, for the X-10 graphite pile, hole 19. Above 1 Mev, however, the ratio is somewhat higher for the LITR, and is 0.056 as compared with 0.034 for the X-10 graphite pile, hole 19. The total integrated flux from 0.1 ev to 1 Mev was found to have a value of 1.05×10^{12} neutrons/cm²·sec.

The high-energy region of the spectrum from approximately 2 to 6 Mev is shown in Fig. 23 with each threshold reaction listed at its respective effective threshold energy. For the purpose of estimating the total integrated number of neutrons per square centimeter above any desired energy, the spectrum is extended to lower energies by using the same plot with the vertical scale multiplied by 10. The total flux is then obtained from the area under the curve.

A Maxwellian density distribution of thermal neutrons based on an experimental measurement of 4.12×10^{12} neutrons/cm²·sec, $(nv)_{th}$ is shown in Fig. 24. Also shown on the same graph is the epithermal neutron density spectrum that follows a $1/E$ law as it approaches the thermal region from the high-energy side.

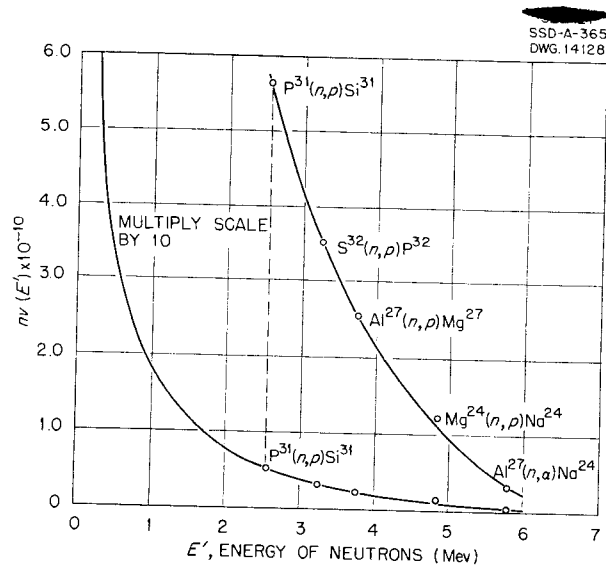


Fig. 23. High Energy Region of Neutron Energy Spectrum in LITR Pneumatic Rabbit Tube.

Figures 25, 26, 27, and 28 are decay curves for various elements used as threshold and resonance detectors.

Figure 25 shows the decay curve for cadmium-enclosed P^{31} bombarded by fast neutrons. The decay curve can be analyzed into two reactions, $P^{31}(n,\gamma)P^{32}$, which decays with a half life of 14.3 days by β^- emission to become stable S^{32} , and $P^{31}(n,p)Si^{31}$, which decays with a half life of 2.7 hr by β^- emission back to P^{31} . The data were obtained with a beta counter standardized with standard P^{32} solution obtained from E. I. Wyatt of the Chemistry Division. Counter efficiencies for Si^{31} betas and P^{32} betas are about equal, since the two beta energies practically coincide.

Figure 26 shows the decay products for aluminum enclosed in cadmium and bombarded with fast neutrons. The decay curves were obtained by measuring the gamma activity with a high-pressure ionization chamber furnished by E. I. Wyatt of the Chemistry Division. This instrument, calibrated in terms of the absolute activities of Co^{60} standards and supplied with data showing its efficiency

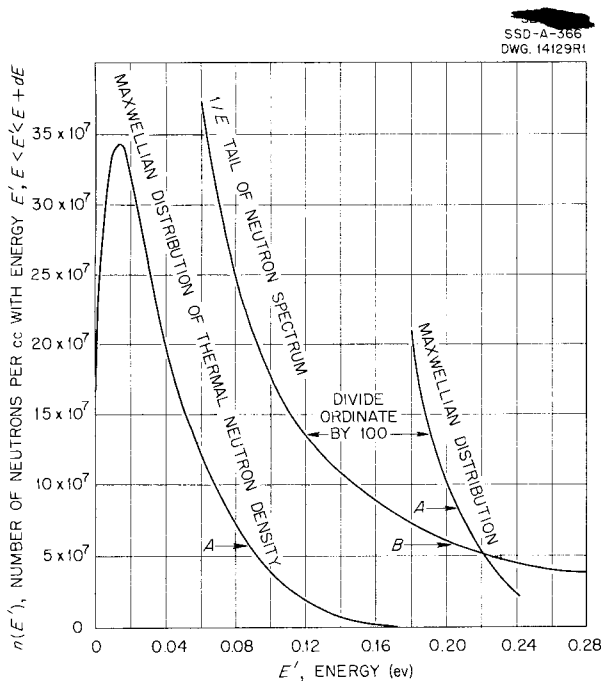


Fig. 24. Two Neutron Density Energy Spectra in LITR.

as a function of gamma energy, was used to obtain the absolute disintegration rate of all irradiated materials yielding radioactive products with well-known decay schemes.

The reaction $Al^{27}(n,\gamma)Al^{28}$ is activated appreciably by resonance absorption of neutrons in the energy region near 9 kev. The curve shown here is for a cadmium-enclosed aluminum sample. This curve, together with one obtained for a bare sample, was used to obtain the cadmium ratio that was then used to compute the energy spectrum around this region, i.e., 9100 ev, the location of the resonance on the cross-section curve.

The reaction $Al^{27}(n,\alpha)Na^{24}$ has an effective threshold at 5.75 Mev and was used to obtain the integrated flux above this energy. Another reaction, $Al^{27}(n,p)Mg^{27}$, with a threshold at 3.75 Mev, was used for this energy region.

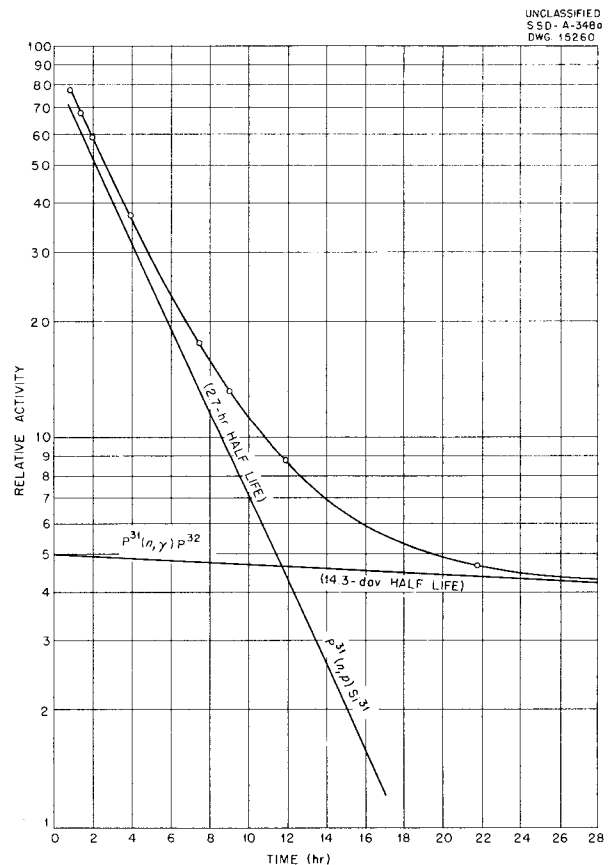


Fig. 25. Decay Curves for P^{32} and Si^{31} from P^{31} .

SOLID STATE DIVISION QUARTERLY PROGRESS REPORT

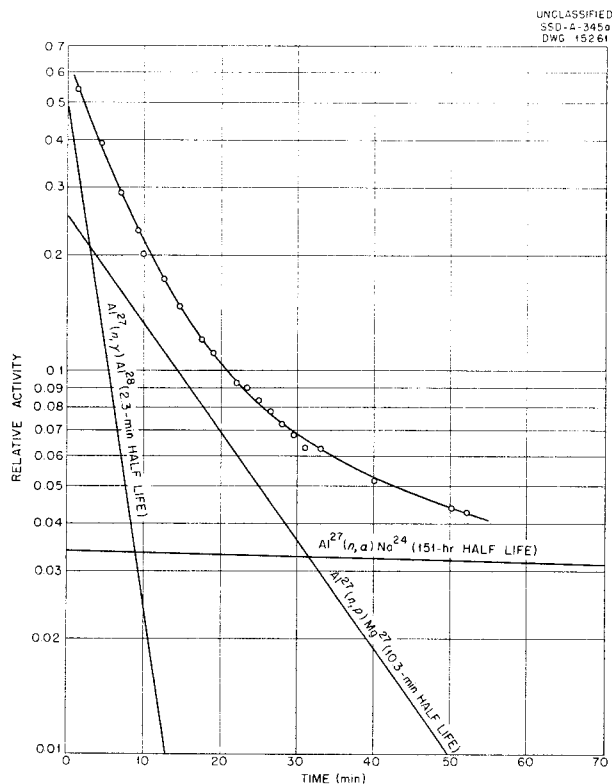


Fig. 26. Decay Curves for Al^{28} , Mg^{27} , and Na^{24} from Al^{27} .

Figure 27 shows the analysis of irradiated NaCl into its two components, Na^{24} with a 15.1-hr period and Cl^{38} with a 38.5-min period. These two (n,γ) reactions were used for the determination of the spectrum at their resonance energies, i.e., 1710 and 1800 ev.

Figure 28 shows the decay curve of 3.8-min vanadium irradiated as V_2O_5 . The purity of the powder is illustrated by its decay curve, which passes through ten half-periods before starting to deviate appreciably from the 3.8-min period.

Tables 4 and 5 are respective summaries of data used to measure the high-energy region and the

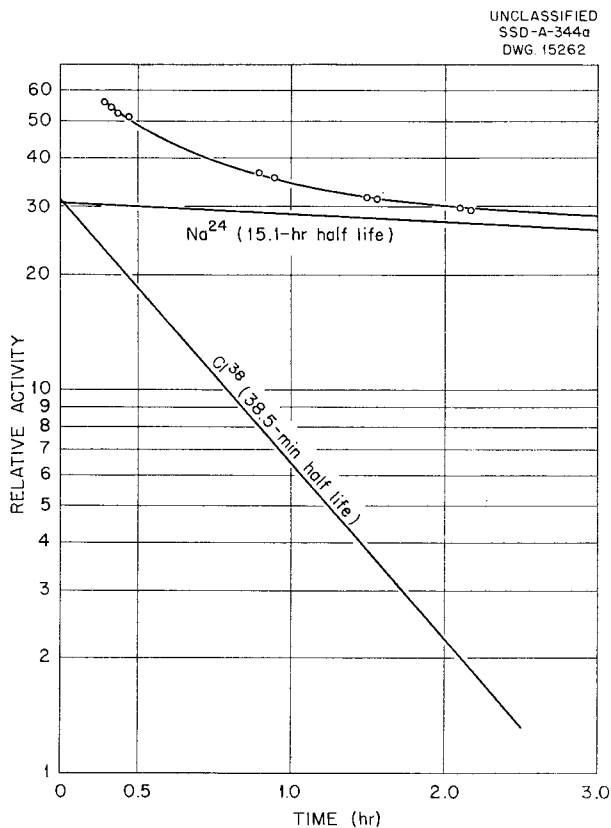


Fig. 27. Decay Curves for Na^{24} and Cl^{38} from $Na^{23}Cl^{37}$.

low-energy region of the spectrum. The data listed for each reaction in Table 4 represent the average of three or four determinations, with the exception of the reaction $Al^{27}(n,p)Mg^{27}$, for which only one decay curve was recorded. Agreement between the determinations was excellent, with most deviations less than 10% between separate successive measurements. The data in Table 5 represent one determination (complete decay curve) for each substance used. However, the uncertainty here is small because reactions are more definite and interference from side nuclear reactions is negligible.

UNCLASSIFIED
 SSD - A-343a
 DWG. 15263

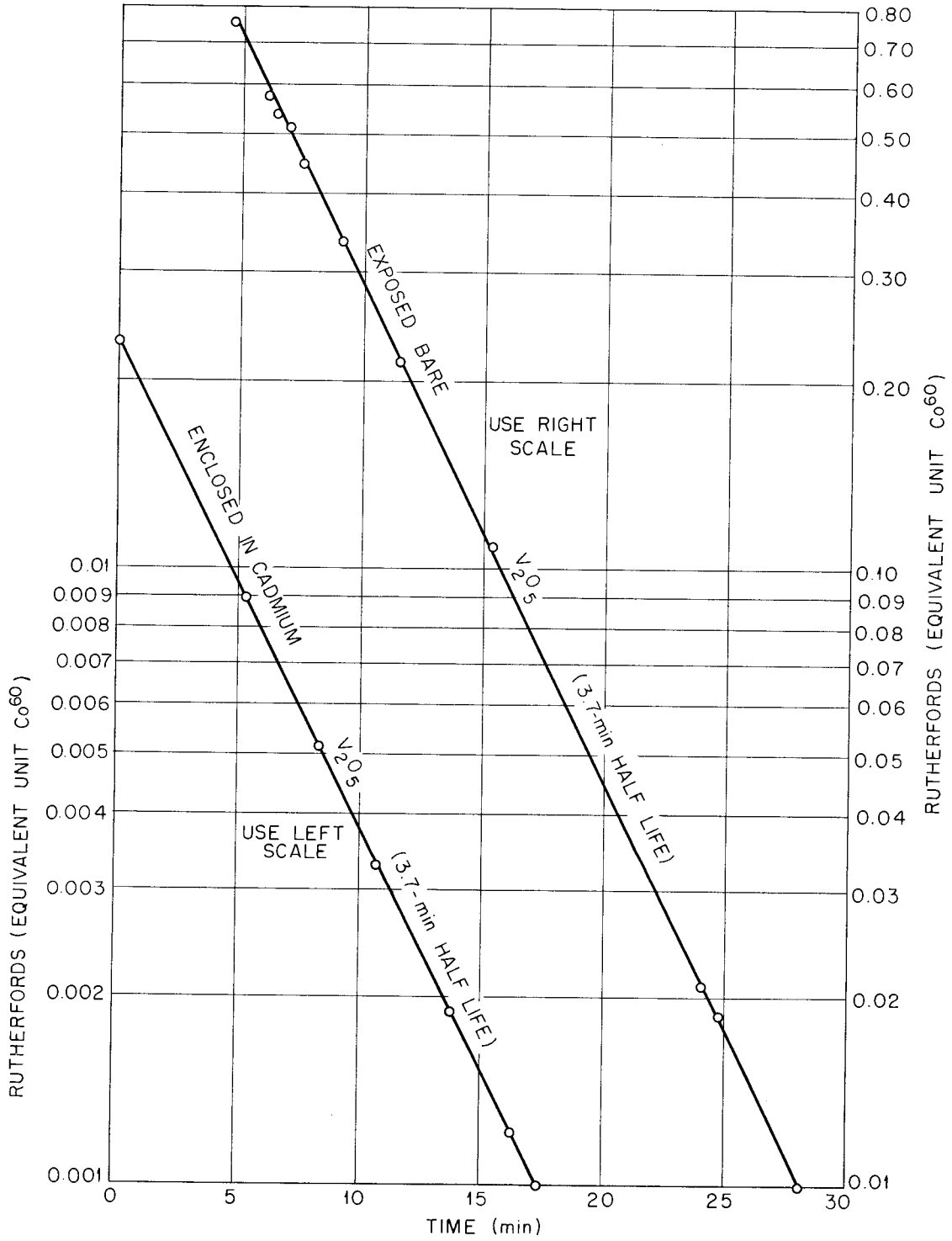


Fig. 28. Decay Curves for Y^{52} .

SOLID STATE DIVISION QUARTERLY PROGRESS REPORT

Table 4

SUMMARY OF NEUTRON SPECTRUM DATA MEASURED WITH THRESHOLD DETECTORS*

Threshold Reaction	Cross Section, σ (barns)	Effective Threshold (Mev)	Flux above Threshold (nv)	$nv(E')dE$ at Threshold Energy (Effective)
$P^{31}(n,p)Si^{31}$	0.071	2.5	8.35×10^{10}	5.7×10^{10}
$S^{32}(n,p)P^{32}$	0.22	3.5	4.77×10^{10}	3.5×10^{10}
$Al^{27}(n,p)Mg^{27}$	0.020	3.8	3.49×10^{10}	2.5×10^{10}
$Mg^{24}(n,p)Na^{24}$	0.024	4.8	1.26×10^{10}	1.3×10^{10}
$Al^{27}(n,\alpha)Na^{24}$	0.048	5.8	0.36×10^{10}	0.6×10^{10}

*Thermal neutron flux, 4.12×10^{12} neutrons/cm²·sec.

Table 5

SUMMARY OF NEUTRON SPECTRUM DATA MEASURED WITH RESONANCE DETECTORS*

Resonance Reaction	Cadmium Ratio	Position of Resonance on Energy Scale (ev)	$nv(E)dE$ (neutrons/cm ² ·sec·Mev)
$Mn^{55}(n,\gamma)Mn^{56}$	44.5	261	2.51×10^{14}
$Na^{24}(n,\gamma)Na^{24}$	66.0	1710	4.82×10^{13}
$Cl^{37}(n,\gamma)Cl^{38}$	73.3	1800	4.73×10^{13}
$V^{51}(n,\gamma)V^{52}$	76.8	3370	2.28×10^{13}
$Al^{27}(n,\gamma)Al^{28}$	80.0	9100	7.97×10^{12}

*Thermal neutron flux, 4.12×10^{12} neutrons/cm²·sec.

LIQUID FUELS

RADIATION DAMAGE TO LIQUID FUELS

G. W. Keilholtz C. C. Webster
 J. G. Morgan P. R. Klein
 H. E. Robertson B. W. Kinyon
 M. J. Feldman

LITR Facility for Liquid-Fuel Exposure. The liquid fuels testing program was concentrated on

experiments in the LITR during this quarter. The facility in use is one that was made by boring a vertical hole in beryllium piece number C-48. The thermal flux in this hole was measured in two positions on a vertical line by using the cobalt activation method. Foils were irradiated for 21.5 hr and then were removed and counted with a high-pressure ionization chamber. During the irradiation the reactor power level was 700 kw. Flux values

obtained were 1.05×10^{13} neutrons/cm²·sec at a point 8.5 in. below the reactor center line and 1.22×10^{13} neutrons/cm²·sec at 3 in. below the reactor center line. When the pile is operated at 800 kw, the flux is estimated to be 1.2×10^{13} at the sample location by assuming that the flux is proportional to reactor power.

All tests were run in capsules with a heater assembly as shown in view (1) of Fig. 29. A basic capsule unit (2) is also pictured with interchangeable caps (3). In measuring pressure during irradiation the two-hole cap is used; one hole accommodates the thermocouple well, and the other connects to the capillary pressure tubing. The one-hole cap is used for static corrosion tests. The thermocouple well and the tubing connector are shown below the capsule proper. The cap is sealed after loading by a heliarc weld.

Potassium Hydroxide Screening Test. A screening test of KOH was made to determine whether excessive pressure would develop under irradiation. The first test in hole 12 of the X-10 graphite pile at a flux of 8.0×10^{11} showed no pressure increase as a result of radiation (Fig. 30).

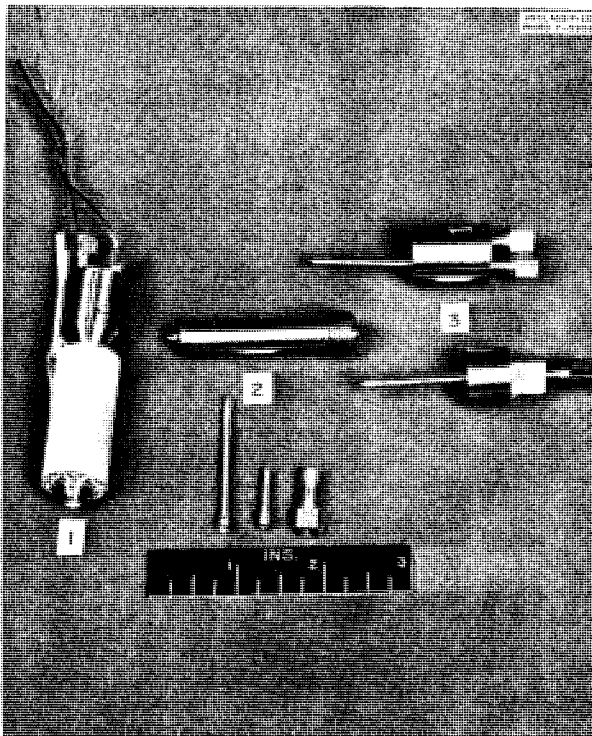


Fig. 29. Capsule and Heater Assembly.

A freshly prepared KOH sample of high purity (less than 0.3% K₂CO₃ and less than 0.2% H₂O) was then tested in the LITR at a flux of 1.2×10^{13} . The pressure increased approximately 3 psi (see Fig. 31), but a duplicate run on the bench without radiation produced a corresponding increase in pressure (see Fig. 32). Calculation of the dissociation of water vapor into hydrogen and oxygen gas for 0.2% H₂O in the sample would cause a pressure of 4 lb in the system. The small pressure increase could be a result of the water content of the KOH.

Test on Reactor Fuel No. 2. Reactor fuel No. 2 was tested in an inconel capsule. This fuel is composed of 46.5 mole % NaF, 26.0 mole % KF, and 27.5 mole % UF₄. Previous tests in the X-10 graphite pile and in the 86-in. cyclotron on this fuel indicated no significant evidence of radiation damage. However, after this eutectic mixture was inserted into the LITR for 115 hr, an increase in corrosion over previous tests by a factor of 10 was indicated when corrosion was determined by chemical analysis and by factors of 3 to 6 when determined by metallographic examination. This means an increase in corrosion from 1 mil in the X-10 graphite pile to 3 mils in the LITR, which may be accounted for by the differences in dissipation of energy: 65 w/cc in the X-10 graphite pile, an average of 300 w/cc in the cyclotron, and 800 w/cc in the LITR.

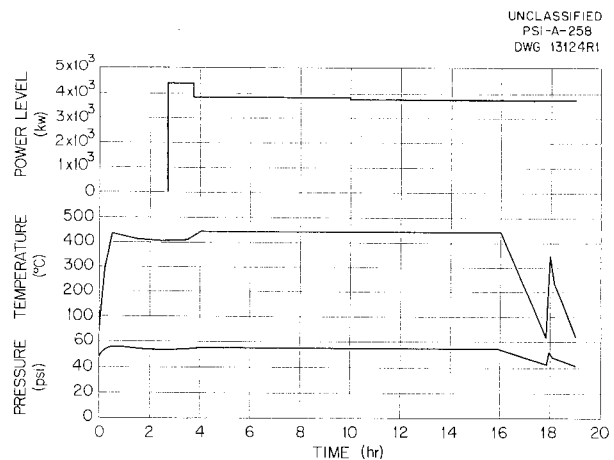


Fig. 30. Temperature and Radiation Effect on Pressure of Potassium Hydroxide in X-10 Graphite Pile, Hole 12.

SOLID STATE DIVISION QUARTERLY PROGRESS REPORT

UNCLASSIFIED
SSD - A-332
DWG. 15264

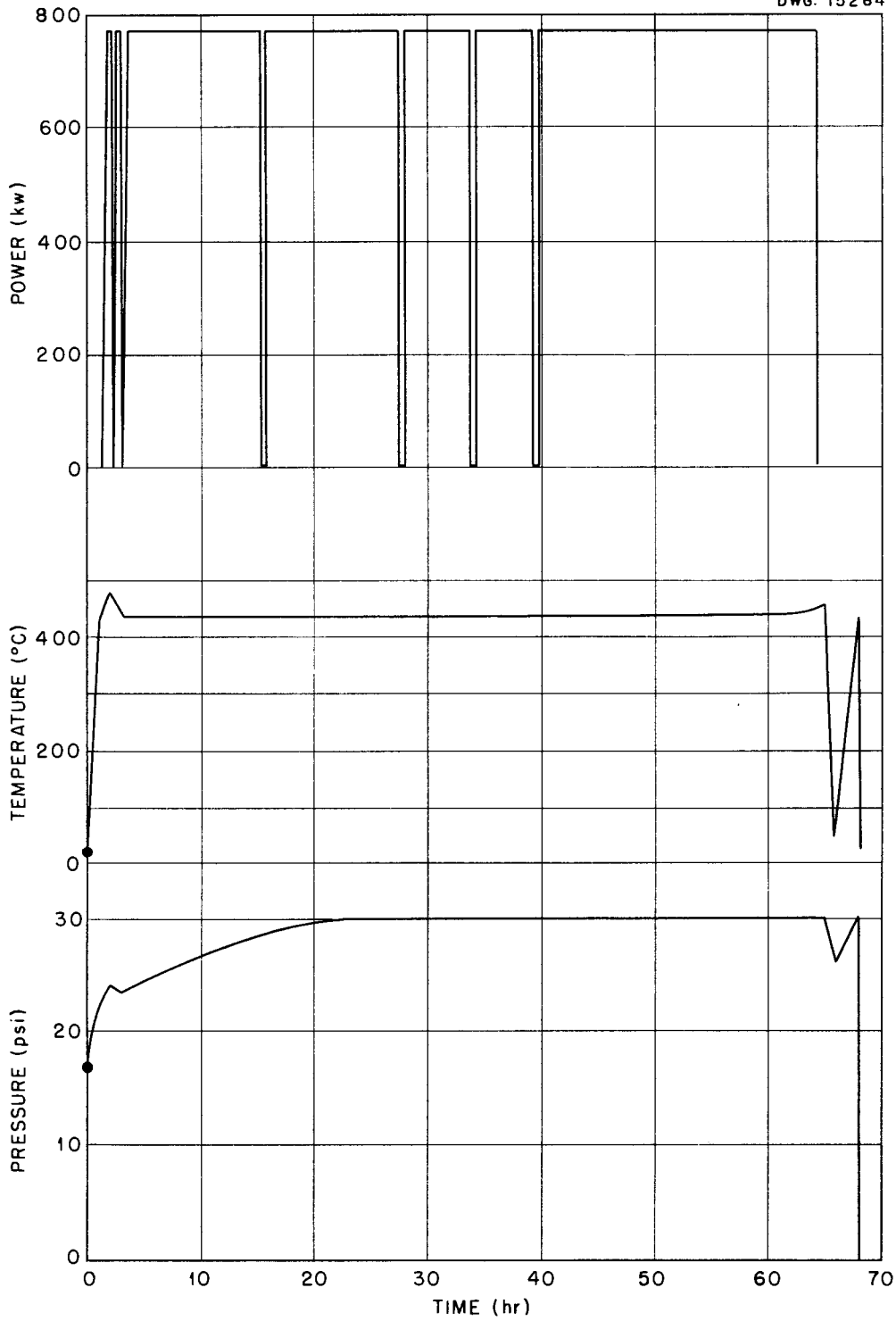


Fig. 31. Potassium Hydroxide in Type-316 Stainless Steel Capsule Under Irradiation.

No pressure effects have been observed in the No. 2 reactor fuel during radiation.

Figure 33 is a metallographic photograph (300x) of the interface of a capsule and No. 2 reactor fuel exposed in the X-10 graphite pile at 1.0×10^{12} neutrons/cm² for 299 hr at 1500°F. The sample shows an intergranular type of attack and a maximum penetration of the order of 1 mil (0.001 in.). The corrosion in the salt end of the capsule is denser than that in the vapor region.

Figure 34 shows an entirely different type of attack after exposure in the LITR at 1.2×10^{13} neutrons/cm² for 115 hr at 1500°F. In addition to the intergranular corrosion, a second type of corrosion is present which appears to have originated at the grain faces on the corrosion interface and proceeds into the grain. This second type of corrosion shows evidence of being preferential in grains attacked and seems to be confined within the grain boundaries of the grain attacked.

The depth of corrosion was measured by using the filar ocular of a Tukon hardness-testing machine. The corrosion interface was taken as the original metal face, and the maximum penetration

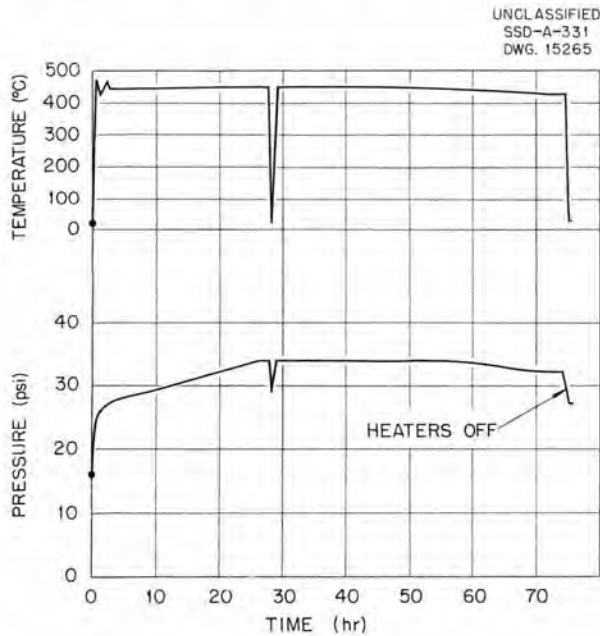


Fig. 32. Potassium Hydroxide in Type-316 Stainless Steel Capsule Unirradiated.

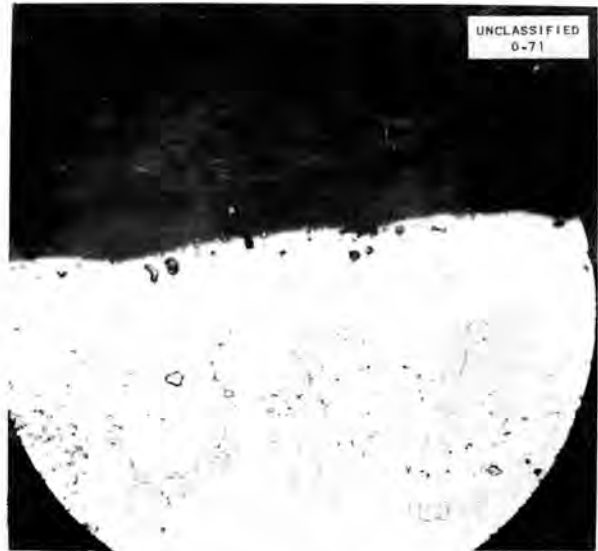


Fig. 33. Metallograph of No. 2 Reactor Fuel Capsule Exposed in X-10 Graphite Pile. Exposure: 1.0×10^{12} neutrons/cm²·sec, 299 hr, 1500°F, 300x. Reduced 24%.

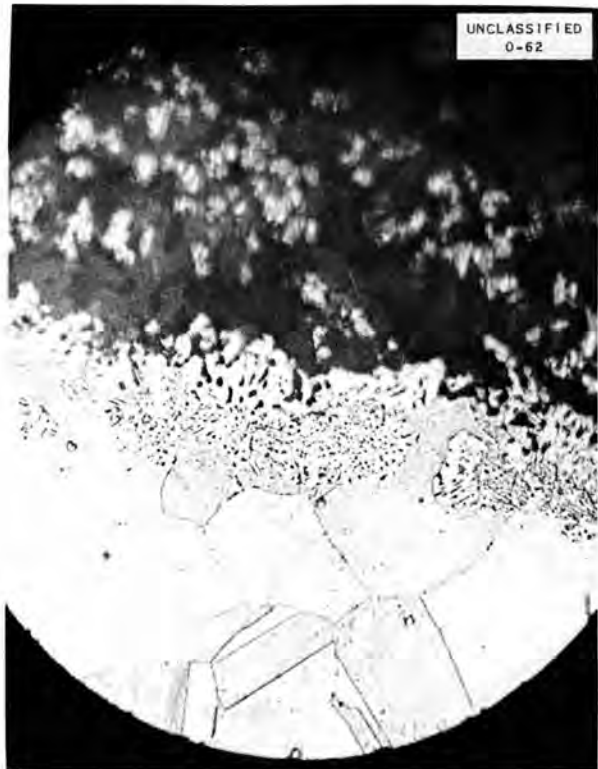


Fig. 34. Metallograph of No. 2 Reactor Fuel Capsule Exposed in LITR. Exposure: 1.2×10^{13} neutrons/cm²·sec, 115 hr, 1500°F, 300x. Reduced 11%.

SOLID STATE DIVISION QUARTERLY PROGRESS REPORT

was measured in a number of places. The penetration varied from 2 mils (0.002 in.) to a maximum of 3 mils (0.003 in.).

The relative density of corrosion was measured by noting the number of grains attacked per number of grains observable on that portion of the interface within the field of the microscope. In general, the salt portion of the capsule showed three to five grains of a six-grain area to be corroded. The area above the salt varied from two to four grains attacked per six-grain field to many areas where nearly all of the grains were attacked, although no portions showed a continuous attack for any great length.

The control samples show a very small amount of intergranular attack. Chemical analysis of the No. 2 fuel is given in Table 6.

Tests on Reactor Fuels Nos. 3 and 17. Reactor fuels No. 3 (60 mole % BeF_2 , 25 mole % NaF , and

15 mole % UF_4) and No. 17 (51 mole % BeF_2 , 47 mole % NaF , and 2 mole % UF_4) have been exposed in the LITR hole C-48 in excess of 100 hr at 1500°F. The average flux of these tests was 1.2×10^{13} neutrons/cm²·sec. Analytical and metallurgical examinations are in process.

Mockup for MTR Tests. A mockup of the equipment required to expose reactor fuels at 3000 w/cc in the MTR is being fabricated for pretesting in the LITR. Under the higher flux of the MTR it will be possible to test salts generating 3000 w/cc. Bench tests have shown that this heat can be dissipated by using air forced past the capsule at a high velocity. The salt temperature is controlled by regulating the cooling air flow by the capsule. A similar test will be conducted first in the top hole of the LITR in order to check the MTR design and instrumentation. The increased fission heat at the lower flux will be reached by using a salt of a higher uranium concentration.

Table 6

TESTS ON REACTOR FUEL NO. 2

Sample No.	Total Time at 1500°F (hr)	Average Flux (neutrons/cm ²)	Heat (w/cc)	Chemical Analysis					Remarks
				U (%)	F (%)	Fe (ppm)	Ni (ppm)	Cr (ppm)	
21	115	1.2×10^{13}	800	70.5		16,329	26,878	1878	Liquid during radiation
22	115	None		51.3		1,270	1,034	754	Liquid without radiation
23	161	1.2×10^{13}	800	56.4	33.4 31.9	6,414	45,169	950	Liquid during radiation
24	164	None		51.0	30.6 27.7	2,655	1,100	645	Liquid without radiation
25	(136 at 440°C)	1.2×10^{13}	800	48.9		1,220	1,380	160	Solid during radiation

CRYSTAL PHYSICS

Y-12 CYCLOTRON RADIATION
DAMAGE STUDIES

W. J. Sturm D. Binder⁽¹⁾
M. J. Feldman R. J. Jones⁽¹⁾

Efforts have been directed, as in previous months, toward the measurement of radiation effects on liquid fuel coolants in container materials of interest for the ANP reactor. Protons of 20 Mev energy from the 86-in. cyclotron at Y-12 have been used exclusively in these experiments. Although cyclotron operation has been stopped for maintenance and repair work for seven weeks, results have been obtained on a few of the 35 samples studied during the last quarter.

Bombardments were performed on water-cooled targets representing five systems: (1) KOH in inconel, (2) KOH in type-316 stainless steel, (3) No. 2 eutectic (27 mole % UF_4) in inconel, (4) LiF eutectic (1.1 mole % UF_4) in inconel, and (5) LiF eutectic in an inconel microcapsule. The last is a simple modification of the No. 4 system carried out in an effort to obtain more homogeneous bombardment conditions. Since work on the 27 mole % eutectic (1.1 mole % UF_4) has been carried as far as is presently planned, a report on this phase of the work is in preparation and will be issued as part of a joint report with the ANP pile radiation-damage group.

Potassium Hydroxide Proton Bombardments.

Two bombardments of KOH in 0.010-in. inconel tubing and five bombardments of KOH in type-316 stainless steel were made. In all cases the irradiations were performed by using large (5-in.) lengths of metal tubing and by bombarding about 2 in. of the length. Because of the possibility of a nonuniform proton beam over this length, it is not possible to ascertain whether temperatures locally exceeded the values given by about 50°C. Under these circumstances, however, it was not possible to bombard either of these systems for 1 hr with 2 to 3 μa of protons at temperatures in excess of 650°C without causing them to corrode

through their 0.010-in. containers; this temperature is about 200°C less than the desired working temperature of 815°C.

Uranium Tetrafluoride Eutectic Proton Bombardments. The bombardments of UF_4 eutectics in inconel were made in either of two types of inconel containers. The standard target, which has been used for all previous work, is a flattened section of 0.250-in.-OD inconel tubing having a 0.010-in. wall; the over-all length of this target is about 5 in. and the bombarded length is about 2 inches. A recent modification, the microcapsule, is similarly made of the same flattened tubing stock but has an over-all length of but 2 in. and a bombarded length of 3/8 inch. Limitation of the bombarded area is expected to make temperature control in the smaller region more precise and to result in fewer target failures as a result of overheating. Since better temperature control is possible with the microcapsule, longer bombardments (8 hr and more) have a reasonable chance of successful completion.

The 28 fuel elements presently being studied are divided into three groups: (1) the 27 mole % UF_4 eutectic (A-2) in the standard inconel container, (2) the 1.1 mole % UF_4 eutectic (containing lithium) in the standard inconel container, and (3) the 1.1 mole % UF_4 eutectic in inconel microcapsules. In each group several bombardments were made of 1-, 2-, 4-, and 8-hr durations. Specific energy input varied from about 100 to 400 w per cubic centimeter of eutectic. The volume of eutectic used for each bombardment was 1.5 cc in the case of the standard capsule and 0.5 cc for the microspecimens.

One member of the third group of targets was a microcapsule that had been heat-treated before bombardment in such a manner as to produce large-grained inconel. This target was filled with eutectic and bombarded for 2 hr with 20-Mev protons (about 150 w per cubic centimeter of eutectic as determined by cooling water inlet and outlet temperatures) in an attempt to enhance intergranular corrosion. A similarly treated unbombarded sample served as a control.

⁽¹⁾Y-12 cyclotron group.

SOLID STATE DIVISION QUARTERLY PROGRESS REPORT

In another case one of the dilute eutectic targets was mounted on a thermally insulated 1-in. block of stainless steel; this was done in an effort to maintain the unbombarded face of the fuel element at a temperature higher than the melting point of the eutectic. Thus it might be expected that small thermal convection loops would be set up in such a way as to increase the effective thermal conductivity of the eutectic by permitting better heat transfer to the cooling water stream and consequent higher proton radiation densities. This was not the case, however, as the specific energy input for this target was the lowest obtained in the series.

Chemical analysis of the bombarded targets and their control samples is still incomplete, and metallurgical study has merely begun; therefore it is not possible to discuss any results at this time.

CORRELATION OF NEUTRON BOMBARDMENT WITH PROTON BOMBARDMENT

W. J. Sturm	D. Binder
M. J. Feldman	R. J. Jones

Bombardments have been made in an effort to obtain an approximate correlation between the effectiveness of protons and pile neutrons for certain types of radiation damage effects. The work of T. H. Blewitt has shown that one approach to this problem is an examination of the plastic properties of copper. In particular, his work has shown that the critical shear stress in a single copper crystal is sensitive to reactor radiations. To pursue these ideas in a convenient yet rapid fashion, work was done on polycrystalline, instead of crystalline, copper. The property analogous to critical shear in crystalline material is the elastic limit, and this has also been shown by Blewitt to be sensitive to radiation.

After some preliminary bombardments it was decided that the A-1 head and base would be a suitable bombardment chamber. The A-1 head is constructed entirely of aluminum with a 0.010-in. window milled out where the beam enters. The

target is held with a spring clamp against the window, and the cooling water runs directly behind the target. This had the advantage of making possible the most efficient cooling and had the disadvantage that no provision was made at the time for thermocouple leads into the target. Also, there was the disadvantage that the current received by the target had to be estimated by known beam distributions on the A-1 head.

For the first run two identical polycrystalline copper tensile specimens, 16 mils thick, were annealed at 1000°C. One was irradiated for an estimated $2.5 \mu\text{a-hr/cm}^2$, while the other was retained as a control. The elastic limit was 4.6 kg/mm² for the irradiated sample as compared with 1.1 kg/mm² for the unirradiated sample.

In the second run the possibility that the former two samples did not have the same tensile history was investigated. Two specimens annealed under the same conditions as those of the first run were used; one specimen was irradiated for an estimated $5 \mu\text{a-hr/cm}^2$, and the second one was mounted behind the first. The two specimens were separated with an aluminum absorber thick enough to stop the beam. Unfortunately, the grip ends of the control specimen were bent by the cooling water, and the combined effects of water pressure and bending increased the observed elastic limit from 1.1 to 1.8 kg/mm². The value for the irradiated sample was 5.4 kg/mm².

Polycrystalline specimens irradiated at 1×10^{18} nvt in the X-10 graphite pile were observed by Blewitt to increase the elastic limit by a factor of 2.5. His data on pure crystals indicate a roughly linear increase in the factor of 1×10^{18} nvt when saturation sets in. Although more measurements should be taken, it would be presumed from the cyclotron data that saturation sets in at about $2.5 \mu\text{a-hr/cm}^2$. Furthermore, a good control value would be an average of unmounted and mounted control samples of 1.5 kg/mm². Then a logical value for comparison with pile data is $2.5 \mu\text{a-hr/cm}^2$, which causes a change by a factor of 3.1 (with about 50% error) in the elastic limit. Thus, experimentally, 1×10^{18} nvt corresponds to $2 \mu\text{a-hr/cm}^2$.

Seitz's calculations⁽²⁾ make use of a critical point at which elastic energy transfers equal ionization and excitation transfers. In copper this occurs for 800-kev recoils or 26-Mev neutrons, which represent more energy than can be obtained in pile irradiations. Preliminary results of a recalculation using a $1/E$ spectrum and certain averaging processes indicate 1×10^{18} nvt = $0.5 \mu\text{a-hr/cm}^2$, which agrees within the limits of error with the foregoing results.

A further result of these calculations shows that the high-energy neutrons of the pile per unit energy range contribute about as much to atomic displacements as the low-energy epithermal neutrons. This follows, since the energy transferred by the neutron (all in elastic collisions) varies as E and the flux as $1/E$, the collision cross section remains comparatively constant, and the fraction of energy lost by the recoils to displacements is also comparatively constant. Neutrons from a (p,n) reaction should then be more effective per unit flux than pile neutrons. Consequently, another experiment was performed in which an irradiation using (p,n) neutrons led to an elastic limit change by a factor of 1.7 for an estimated 10^{16} nvt and showed an advantage of approximately 60 times (again per unit flux) that of a pile bombardment.

The well-known conclusion that comparatively modest beam currents produce radiation damage effects (which depend on displacements) many times faster than pile irradiations is substantiated. Using a rough correlation of 1×10^{18} nvt = $2 \mu\text{a-hr/cm}^2$, $25 \mu\text{a/cm}^2$ irradiations would produce effects 1000 times as fast as the X-10 graphite pile and 60 times as fast as the LITR. Furthermore, if the inherently more manageable neutron irradiations are preferred, fast neutrons from beryllium targets may be used at least as effectively as the LITR.

X-RAY WORK

G. E. Klein F. A. Sherrill

A total of 141 diffraction patterns were recorded during the quarter, 99 of which were made of

(2) F. Seitz, "The Influence of Pile Radiations on Solid Materials," *Journal of Metallurgy and Ceramics*, TID-65, p. 142 (July 1948).

copper single-crystal test specimens photographed by the back-reflection Laue method for determining their orientation. Miscellaneous powder and single-crystal samples were analyzed for identification purposes.

X-ray diffraction studies were made of lithium fluoride crystals before and after neutron irradiation to determine (1) whether any structural change was induced by the irradiation, (2) whether only the lattice dimensions changed, or (3) whether no change at all was observed by x-ray diffraction methods.

Powder patterns that were taken indicated no change in structure after irradiation and also no change in lattice parameter. Reflections from the (200) and (400) planes of single crystals used with the North American Philips spectrometer before and after irradiation indicated no observable change in lattice parameter. While in the process of using the spectrometer for observing the lattice parameters of the lithium fluoride crystals, other lines that at first were thought to be caused by the neutron irradiation of lithium fluoride also appeared. It was found, however, that these lines were caused by wave lengths produced by other metals in or on the copper target of the x-ray tube. This in no way destroys the usefulness of a particular sealed-off tube target, since these other lines are so weak compared with the expected lines that they can be distinguished from the normally expected lines. These other lines can probably be expected from any spectrometer with high-intensity x rays and good alignment when work is done with a strongly diffracting crystal such as lithium fluoride or mica. As a check on this conclusion the crystals were exposed by the Metallurgy Division in their two diffraction units in which copper targets were used; the same phenomena were observed. The iron trace comes either directly from the target or from the slit system.

Single crystals of beryllium-copper and quartz were annealed and examined before and after irradiation to determine what structural changes, if any, are produced by irradiation.

Cu_3Au wires were examined for order-disorder phenomenon, and the grain size caused by ordering was determined. The data will be correlated with values theoretically obtained by T. H. Blewitt.

SOLID STATE DIVISION QUARTERLY PROGRESS REPORT

Attempts to operate the G-E x-ray tube for the hot cell spectrometer and the North American Philips diffraction tube, in which the output of the Hilger unit was used, were not entirely successful. Since the Hilger unit supplies high a-c voltage and sealed-off diffraction tubes require high d-c voltage, electrical difficulties became evident at an early stage in the operation. The current output of the Hilger unit also proved to be too irregular for successful operation of the Philips spectrometer. The spectrometer requires a constant output of x-ray energy so as to provide a reproducible set of conditions during operation. Installation of a North American Philips diffraction unit should remedy both of the existing difficulties. The Philips unit is expected to arrive in time to be placed in operation by mid-February.

Semi-quantitative determinations of specific gravity values in the range of 1.2 to 7.5, inclusive, can now be made with the use of heavy index liquids received during the quarter.

A simplified apparatus has been constructed for studying the small-angle scattering by materials. The experimental procedure consists in passing a monochromatized x-ray beam through a thin foil of the single crystal and allowing the divergent beam to travel through a 3-ft long evacuated tube to impinge on an x-ray film at the end of the tube. The refraction caused by precipitate nuclei results in the x-ray beam divergence that can be measured on the film. The first problem to be studied is the small-angle scattering from copper-beryllium specimens. An attempt will be made to obtain direct evidence of the formation of precipitate nuclei after irradiation of the copper-beryllium alloy.

The level of general scattered radiation in the vicinity of the hot cells has created a problem in the successful operation of equipment in the x-ray diffraction laboratory. The level of approximately 1000 counts/min necessitates the shielding of the Geiger counter tube with a considerable thickness of lead in order to reduce the background to nearly tolerable amounts. Films cannot be stored in the vicinity of the x-ray laboratory, and exposed films must be processed immediately to reduce the effects of extraneous irradiation as much as possible. It may be necessary to move the location of

all but the hot-cell spectrometer unless a satisfactory remedy to the situation can be effected.

THERMAL CONDUCTIVITY OF STRUCTURAL MATERIALS

A. Foner Cohen L. C. Templeton

Further experiments in measuring thermal conductivity changes in inconel have been performed in the X-10 graphite pile. At temperatures up to and including 575°C no change in conductivity was observed over a period of two months. However, at a temperature of approximately 820°C a decrease in conductivity was observed. Work is in progress to determine the possible reasons for such behavior. It is believed that the heat treatment of the alloy is an important factor.

Additional experiments with inconel are in progress in the LITR. At present an inconel specimen which has been stabilized with respect to carbide precipitation for temperatures up to 850°C is in the LITR. The thermal conductivity in this experiment is measured by an absolute method.

A high-purity, cobalt-free nickel specimen that was vacuum-annealed before testing has been used in experiments in which changes in thermal conductivity were measured. As reported in the last quarterly,⁽³⁾ no appreciable change in thermal conductivity was observed at temperatures up to 200°C in the X-10 graphite pile. The same specimen has since been subjected to testing at approximately 820°C. Irradiation of several weeks caused no change in this property.

An absolute thermal conductivity experiment with type-316 stainless steel as the test specimen was run at 250°C in the LITR at a power level of approximately 800 kw for a period of about one month. No change in the thermal conductivity as a function of irradiation time was observed. The nuclear heating in type-316 stainless steel in hole HB-3 of the LITR was calculated from the experimental data to be about 0.04 cal/g. sec.

⁽³⁾A. F. Cohen, "Thermal Conductivity of Structural Materials," *Physics of Solids Quarterly Progress Report for Period Ending October 31, 1951*, ORNL-1214, p. 59.

SPECIAL PROJECTS

TESTS ON GRAPHITE-URANIUM OXIDE BARS

R. H. Kernohan

Preirradiation measurements of weight, modulus of elasticity, relative thermal conductivity, and electrical resistivity have been made on the graphite-uranium oxide test bars⁽¹⁾ fabricated by Battelle Memorial Institute.

The test bars are made of resin-bonded molded graphite baked at 2500°F (not graphitized) and contain 5% uranium by weight (3% by volume) in the form of UO₂ nodules sized as listed in Table 7. The bars are rectangular in shape, approximately 0.230 by 0.296 by 2.86 in., and weigh about 5.5 grams.

⁽¹⁾R. H. Kernohan, "Studies of Miscellaneous Materials," *Physics of Solids Quarterly Progress Report for Period Ending October 31, 1951*, ORNL-1214, p. 38.

Eight of the test bars are held in each steel specimen container (Fig. 35), which is inserted in the center of the X-10 graphite pile for one month. The specimens are separated by aluminum spacers, and three thermocouples are located so that they give the maximum and minimum temperatures attained. Each container is made vacuum-tight, pumped down to about 15 μ vacuum, and flushed with dry helium gas several times. A three-month irradiation schedule in hole B of the X-10 graphite pile is as follows:

Container A, Dec. 10 to Jan. 7 (1 month)
 Container B, Jan. 7 to Feb. 4 (1 month)
 Container C, Feb. 4 to March 3 (1 month)

The thermal flux in hole B as measured by a cobalt foil monitor placed in a cavity in the cap of container A was 9×10^{11} neutrons/cm².

The preirradiation measurements of the graphite bars are given in Table 8. The electrical resistivity values are probably the most accurate. The

Table 7

SIZE OF URANIUM OXIDE NODULES IN GRAPHITE-URANIUM OXIDE TEST BARS

Specimen No.	Content	Avg. Particle Size (μ)
S	UO ₂ nodules (93% enriched uranium)	586 \pm 16
T	UO ₂ nodules	334 \pm 6
U	UO ₂ nodules	94 \pm 0.2
V	UO ₂ nodules	<44
X	Same as S (normal uranium)	586 \pm 16
2X	Same as T (normal uranium)	334 \pm 7
3X	Same as U (normal uranium)	94 \pm 0.2
4X	Same as V (normal uranium)	<44
R	No uranium (control specimens)	

SOLID STATE DIVISION QUARTERLY PROGRESS REPORT

modulus of elasticity values were determined by a dynamic method;⁽²⁾ each bar was vibrated at one end, and the vibration was picked up at the other end. The Pickup signal was at a maximum when the bar was vibrating at its natural frequency, from which the modulus of elasticity was determined. Thermal conductivity measurements were relative. A bar was set vertically in a low-melting alloy

⁽²⁾R. H. Kernohan, "Dynamic Modulus Apparatus," *op. cit.*, ORNL-1214, p. 8.

bath at about 160°C, and a thermocouple was pressed against the top of the bar. The difference in temperature between the alloy bath and the top of the bar yields a rough measure of the thermal conductivity.

A specimen of AGOT graphite was measured and irradiated for comparison with the molded graphite. The electrical resistivity was 1125 $\mu\text{ohm-cm}$, Young's modulus was 0.89×10^6 psi, and the ΔT for relative thermal conductivity was 30.5°C.

Table 8

PREIRRADIATION MEASUREMENTS OF GRAPHITE-URANIUM OXIDE TEST BARS

Specimen No.	Young's Modulus ($\times 10^6$) (psi)	Electrical Resistivity at 20°C ($\mu\text{ohm-cm}$)	ΔT , Temperature Difference (°C)
ZZ-1	0.89	1127	40.2
R-1	2.96	1409	61.1
R-2	2.90	1432	64.5
R-6	2.90	1444	66.7
S-5	2.90	1401	68.1
S-12	2.87	1437	71.8
S-9	2.85	1421	69.2
T-6	2.85	1399	62.0
T-17	2.87	1419	69.5
T-2	2.87	1430	64.3
U-7	2.92	1404	66.0
U-4	2.90	1459	70.6
U-11	2.93	1430	67.0
V-3	2.82	1503	67.8
V-7	2.75	1509	75.8
V-8	2.80	1510	68.8
X-10	2.39	1612	69.0
X-4	2.70	1525	76.2
2X-8	2.60	1534	73.4
2X-4	2.55	1556	72.9
3X-3	2.39	1612	73.0
3X-6	2.47	1571	69.4
4X-5	2.44	1666	72.7
4X-4	2.45	1637	75.2

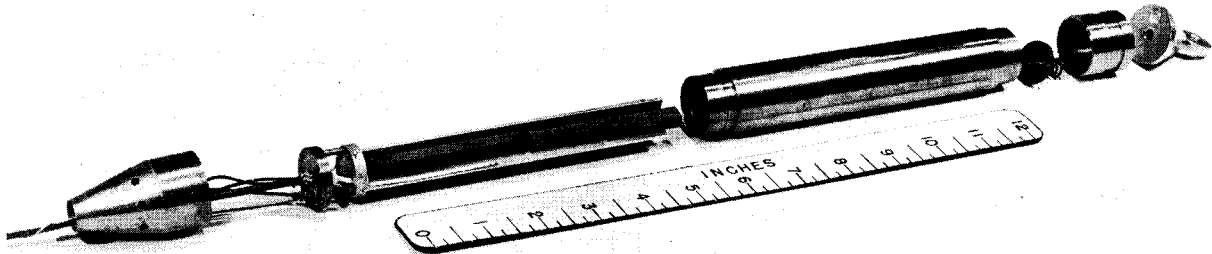


Fig. 35. Graphite-Uranium Oxide Specimen Container.

Measurements on the irradiated specimens from containers A and B are now in progress. A complete report of results should be available next quarter.

ACTIVITY MEASUREMENTS OF SPECIAL MATERIALS

R. H. Kernohan

Rough activity measurements were made on a few materials irradiated at the request of W. M. Hurst of the GE-ANP Physics Division. These materials were weighed and placed in the center of hole 1968 of the X-10 graphite pile on January 2 and were removed January 7; the total neutron irradiation time was 108 hours. The beta and gamma activity was read on a cutie pie held in contact with each specimen. Results are tabulated in Table 9.

IRRADIATION OF DIAMOND CHIPS

R. H. Kernohan J. B. Trice
M. Cines⁽³⁾

An attempt was made to find a metallic matrix material to hold diamond chips for irradiation between the fuel plates in the LITR and possibly in the MTR. This work was done in cooperation with M. Cines. It is hoped that some correlation will be found between the change in the lattice constant of diamond and the integrated fast flux. The problem is that the diamonds are small chips and must fit in a small space. The container must not become too radioactive, and some provision should be made to keep the diamond at pile ambient temperature.

⁽³⁾Phillips Petroleum Company.

Table 9

ACTIVITY MEASUREMENTS ON SPECIAL TEST MATERIALS

Test Material	Activity per Gram of Material After Shutdown (mr/hr)				
	10 hr	30 hr	60 hr	180 hr	225 hr
Grade A lavite	2800	1250	350	40	35
Alumina (38-500), dry pressed, fired	145	55	15	0	0
Alumina, slip molded, fired	310	160	40	3	0
Amber No. 1	90	34	26	22	22
Fused quartz tubing (clear)	225	9	2	2	2
Natural quartz crystal	135	4	2	2	2
Amber No. 2	21	17	15	13	13
Neoprene	1450	1100	650	400	400
2S aluminum	850	320	90	12	0
99.99% pure aluminum	560	225	58	6	3
Platinum foil	$>10^4$	$>10^4$	$>10^4$	9000	9000

An attempt was made to embed the diamond chips in small beads of a low-melting ternary alloy (m.p. = 96°C) consisting of bismuth, lead, and tin. Although the cross sections are low, the extreme toxicity of the decay product of bismuth

(Po^{210}) makes this scheme nearly intolerable in a high-flux reactor.

Other schemes for irradiation will be considered in the near future.